

# The Stellar Content of Active Galaxies

Roberto Cid Fernandes Jr.<sup>1†</sup>, Thaisa Storchi Bergmann<sup>2\*†</sup> and Henrique R. Schmitt<sup>2†‡</sup>

<sup>1</sup> *Departamento de Física, CFM - UFSC, Campus Universitário - Trindade, Caixa Postal: 476. CEP: 88040-900 Florianópolis, SC, Brazil.*

<sup>2</sup> *Instituto de Física - UFRGS, Caixa Postal: 15051. CEP: 91501-970 Porto Alegre, RS, Brazil.*

5 September 2018

## ABSTRACT

We present the results of a long-slit spectroscopic study of 39 active and 3 normal galaxies. Stellar absorption features, continuum colors and their radial variations are analyzed in an effort to characterize the stellar population in these galaxies and detect the presence of a featureless continuum underlying the starlight spectral component. Spatial variations of the equivalent widths of conspicuous absorption lines and continuum colors are detected in most galaxies. Star-forming rings, in particular, leave clear fingerprints in the equivalent widths and color profiles. We find that the stellar populations in the inner regions of active galaxies present a variety of characteristics, and cannot be represented by a single starlight template. Dilution of the stellar lines by an underlying featureless continuum is detected in most broad-lined objects, but little or no dilution is found for the most of the 20 type 2 Seyferts in the sample. Color gradients are also ubiquitous. In particular, all but one of the observed Seyfert 2s are redder at the nucleus than in its immediate vicinity. Possible consequences of these findings are briefly outlined.

**Key words:** galaxies:active; galaxies:nuclei; galaxies:Seyfert; galaxies:stellar content; galaxies:general

## 1 INTRODUCTION

Starlight constitutes a substantial fraction of the light gathered in optical spectra of active galactic nuclei (AGN), particularly in low luminosity objects such as LINERs and Seyfert galaxies, where the stellar component is often dominant. Quantifying and removing the contribution of the stellar population is one of the first and most critical steps in the analysis of AGN spectra, as the shape of the resulting continuum is strongly dependent on the adopted stellar population spectrum.

The most widely used technique for starlight subtraction consists of using an appropriately chosen spectrum of a normal galaxy as a template for the stellar component. The template spectrum is scaled to match as closely as possible the stellar absorption features in the observed spectrum, and the residual after its subtraction is taken as the stellar-free, pure AGN spectrum. This technique has been exten-

sively applied since it was first introduced by Koski (1978), in his early study of Seyfert 2s (e.g., Stauffer 1982, Phillips, Charles & Baldwin 1983, Malkan & Filippenko 1983, Filippenko & Sargent 1988, 1983, Miller & Goodrich 1990, Ho, Filippenko & Sargent 1993, Kay 1994, Tran 1995a). Alternatively, the shape and strength of the starlight component can be estimated by means of stellar population-synthesis techniques. This approach was followed by Keel (1983), who built synthetic templates using a library of stellar spectra plus assumptions about the mass function and star-formation history. Synthetic templates can also be obtained combining a spectral library of star-clusters, a method first used by Bica (1988) in his analysis of the stellar populations of normal galaxies. Bonatto, Bica & Alloin (1989), Storchi-Bergmann, Bica & Pastoriza (1990) used this technique to determine the integrated stellar content of the bulge of active galaxies.

The starlight evaluation procedure yields the stellar and AGN fluxes as a function of wavelength. The AGN spectrum, of course, is not known *a priori*, but the starlight subtraction is usually done in a way to produce a smooth residual continuum. This assumption is based on the fact that the continuum is essentially featureless in objects like bright Seyfert 1s and QSOs, where the AGN component dominates. It is customary to characterize the relative intensity of the starlight and featureless continuum (hereafter

\* Visiting Astronomer, Cerro Tololo Interamerican Observatory, operated by the Association of Universities for Research in Astronomy, Inc., under contract with the National Science Foundation.

† CNPq fellow.

‡ E-mail: cid@fsc.ufsc.br (RCF); thaisa@if.ufrgs.br (TSB); schmitt@if.ufrgs.br (HRS).

FC) components by their fractions ( $f_*$  and  $f_{\text{FC}}$ ) of the total flux at a given wavelength. These fractions depend on the chosen template, the aperture and the actual contrast between the AGN and stellar spectral components. The effect of the FC is to *dilute* the stellar absorption lines in the nuclear spectrum, and it is precisely the degree of dilution with respect to the starlight template which determines  $f_*$  and  $f_{\text{FC}}$ .

In this paper we explore a different approach to estimate the dilution of absorption lines caused by the presence of a FC. Our method makes use of the radial information available through high signal to noise long-slit spectroscopy of a large sample of objects. By studying the variation of the equivalent width ( $W$ ) of conspicuous absorption lines as a function of distance to the nucleus, we are able to determine how much dilution (if any) occurs in the nucleus with respect to extra-nuclear regions, presumably not affected by the FC. In a way, this method amounts to using the off-nucleus spectrum of a galaxy as its own starlight template, a starlight evaluation technique which has been a successfully applied in some previous works (Fosbury et al. 1978, Schmitt, Storchi-Bergmann & Baldwin 1994, Winge et al. 1995, Storchi-Bergmann et al. 1997). Continuum color gradients are also examined, complementing the study of absorption line gradients and bringing in information about the reddening of the nuclear regions.

A second goal of this paper is to provide an homogeneous database for the study of the stellar populations in active galaxies. As discussed above, in previous works the interest in the stellar population has focused in removing its contribution from the nuclear spectrum. The  $W$ s and continuum colors measured in this work allow a characterization of the global properties of the stellar populations as close as a few hundred of parsecs from the nucleus, offering the prospect of a comparative study between the stellar content of normal and active galaxies and between different types of AGN.

This investigation touches upon a number of key issues in current AGN research, such as: (1) the question of starlight evaluation and subtraction techniques; (2) the characterization of the stellar population in active galaxies; and (3) the nature of the FC in Seyfert 2 galaxies and its implications for unified models. In the current paper we focus on the presentation of the data, the analysis of the stellar population features and their radial variations. Future communications will explore the consequences and interpretation of our results in full detail.

This paper is organized as follows. In §2 we present the sample galaxies and describe the observations. The method of analysis (continuum determination and  $W$  measurement) is discussed in §3. The results are presented in §4 and discussed in §5. Finally, §6 summarizes our main results.

## 2 OBSERVATIONS

The sample comprises 20 Seyfert 2s, 6 Seyfert 1s, 7 LINERs and 5 radio galaxies, as well as 4 ‘normal’ nuclei. With the exception of the radio galaxies, all of them are bright nearby objects. Table 1 describes the sample properties. Long-slit spectra of these galaxies have been collected in three epochs using the same technique and instrumentation such that we

have formed an homogeneous database, which can be used for a comparative study of the different kinds of galaxies.

The observations were carried out using the Cassegrain Spectrograph with the 4m telescope of the Cerro Tololo Inter-American Observatory. The spectral range covered is  $\sim 3500\text{--}7000\text{ \AA}$ , at a resolution of  $5\text{--}8\text{ \AA}$ . A slit width corresponding to  $2''$  in the sky was oriented along the position angle (hereafter PA) which allowed the best coverage of the extended emission (although in this work we concentrate on the properties of the continua and stellar absorption features). A log of the observations is presented in Table 2, where we also list the parallactic angle, air mass during the observations, pixel size and spatial scale (evaluated with  $H_0 = 75\text{ km s}^{-1}\text{ Mpc}^{-1}$ ). It can be noticed that, only for a few galaxies, namely 3C33, CGCG420-015 and NGC 4303, the effect of differential refraction is important, displacing the light at  $3700\text{ \AA}$  by  $\sim 1''$  relative to the light at  $5000\text{ \AA}$ , so that some distortion of the continuum slope can be expected in the individual extractions for these objects, if the continuum presents significant variations along the slit. The reduction of the spectra was performed using standard techniques in IRAF. After flux and wavelength calibration, the redshifts were determined from the narrow emission lines present and the spectra were converted to rest-frame units.

The long-slit used corresponded to  $5'$  in the sky, and sky subtraction was performed by the fit of a polynomial to the outer regions of the frame and then subtracting its contribution to the hole frame using the task `background` in IRAF. The most extended galaxies, presenting enough S/N ratio to allow measure the spectral features up to approximately  $100''$ , were NGC1097, the most extended, followed by NGC1672. For these galaxies the sky level adopted may have been overestimated. In order to evaluate an upper limit to the effect, we have compared the flux level of the adopted sky to the flux of the inner regions. We have concluded that its value amounts to less than one percent when compared with the flux of the nucleus, but rising with distance from the nucleus. At approximately  $25''$ , its contribution is about 10%. Assuming that the ‘sky’ flux is actually galaxy flux, the flux level of the sky-subtracted spectrum will be underestimated by at most 10 percent at  $25''$  and more outwards. Thus the measurements of these two galaxies are subjected to this uncertainty farther than  $25''$  from the nucleus. The effect should be negligible for the other less extended galaxies.

One-dimensional spectra were extracted from the two-dimensional frames. The number of extractions varied from 4 for PKS0745-19 to as many as 26 for NGC 1097, totaling 491 spectra for the whole sample. The spatial coverage ranged between  $\pm 3$  and  $\pm 80''$  from the nucleus, while the width of the extractions was typically  $2''$  in the brighter nuclear regions, gradually increasing towards the fainter outer regions to guarantee enough signal. Given that the seeing during the observations was typically  $1.5''$ , some of the narrow extractions are slightly oversampled, resulting in a smoothing of the sharpest spectral variations.

The S/N ratio at  $5650\text{ \AA}$  ranges from  $\sim 5$  to 100, with an average of 40 for all extractions. Even in the blue region, where the noise is usually higher, the spectra are of excellent quality, with a mean S/N ratio of 25 at  $4200\text{ \AA}$ . The high quality of our data has allowed the measurement of stellar population features in spectra extracted up to several kpc's

NAME	ALT. NAME	$\alpha$ (1950)	$\delta$ (1950)	TYPE	MORPH.	$v$	$B_{To}$	$E(B-V)_G$
Mrk 348	NGC 262	00 46 05	31 41 04	2	SA(s)0/a	4669	13.94	0.060
3 C 33	Pks 0106+13	01 06 12	13 02 33	NLRG	E	17230	19.50	0.025
NGC 526a	ESO 352-IG66	01 21 37	-35 19 32	1.9	S0 pec	5762	14.50	0.000
Mrk 573	UGC 1214	01 41 23	02 05 56	2	SAB(rs)0 <sup>+</sup>	5161	13.57	0.008
IC 1816	ESO 355-G25	02 29 48	-36 53 29	2	SA:(r:)a	5086	13.66	0.000
NGC 1097	ESO 416-G20	02 44 11	-30 29 01	Lin-1	SB(rl)b	1193	9.92	0.020
ESO 417-G6	MCG-05-08-006	02 54 18	-32 23 00	2	(R)SA0/a	4792	14.15	0.000
NGC 1326	ESO 357-G026	03 22 01	-36 38 24	Lin	SB(rl)0/a	1244	11.25	0.000
Mrk 607	NGC 1320	03 22 18	-03 13 03	2	Sa:sp	2716	13.31	0.018
NGC 1358	MCG-1-10-003	03 31 11	-05 15 24	2	SAB(r)0/a	3980	12.70	0.025
NGC 1386	ESO 358-G35	03 34 51	-36 09 47	2	SB(s)0 <sup>+</sup>	741	12.12	0.000
NGC 1433	ESO 249-G014	03 40 27	-47 22 48	Lin	SB(rs)ab	920	11.37	0.000
Pks 0349-27	GSP 022	03 49 32	-27 53 29	NLRG	E	19190	16.80	0.000
NGC 1598	ESO 202-G26	04 27 08	-47 53 29	Lin	SAB(s)c	4939	13.44	0.000
NGC 1672	ESO 118-G043	04 44 55	-59 20 18	Lin	SB(r)bc	1155	10.25	0.000
CGCG 420-015		04 50 47	03 58 47	2	E/S0	8811	15.00	0.070
ESO 362-G8	MCG-06-12-009	05 09 20	-34 27 12	2	S0?	4616	13.51	0.005
ESO 362-G18	MCG-05-13-017	05 17 44	-32 42 30	1	S0/a	3603	13.58	0.000
PICTOR A	ESO 252-GA018	05 18 24	-45 49 43	BLRG	SA0 <sup>0</sup> :pec	10308	15.94	0.225
Pks 0634-20	IRAS 06343-2032	06 34 24	-20 32 19	NLRG	E	16320	17.58	0.405
Pks 0745-19		07 45 17	-19 10 15	NLRG	E	35940	18.00	—
Mrk 1210	UGC 4203	08 01 27	05 15 22	2	S?	3910	14.21	0.018
NGC 2935	ESO 565-G23	09 34 26	-20 54 12	Normal	SAB(s)b	2072	11.81	0.028
NGC 3081	ESO 499-IG31	09 57 10	-22 35 06	2	SAB(r)0/a	2164	12.59	0.033
Mrk 732	IC 2637	11 11 14	09 51 33	1.5	E pec	8670	13.89	0.005
IRAS 11215-2806		11 21 35	-28 96 46	2		4047	13.00	0.088
MCG-05-27-013		11 24 55	-28 59 00	2	SB(r)a?	7263	13.71	0.063
NGC 4303	UGC 7420	12 19 22	04 45 03	Lin	SAB(rs)bc	1486	13.68	0.000
MCG-02-33-034		12 49 35	-13 08 36	1		4386	15.00	0.015
FAIRALL 316	ESO 269-G12	12 53 50	-46 39 18	2	S0?	4772	13.81	0.185
NGC 5135	ESO 444-G32	13 22 57	-29 34 26	2-SB	SB(l)ab	3959	12.37	0.058
NGC 5248	UGC 8616	13 35 02	09 08 23	Normal	SAB(rs)bc	1128	10.63	0.000
NGC 5643	ESO 272-G16	14 29 28	-43 57 12	2	SAB(rs)c	1066	10.23	0.125
NGC 6221	ESO 138-G03	16 48 26	-59 08 00	SB	SB(s)bc pec	1368	9.77	0.220
NGC 6300	ESO 101-G25	17 12 18	-62 45 54	2	SB(rs)b	997	10.20	0.120
NGC 6814	MCG-02-50-001	19 39 56	-10 26 33	1	SAB(rs)bc	1676	10.96	0.150
IC 4889	ESO 185-G14	19 41 18	-54 27 54	Normal	E	2473	12.06	0.045
NGC 6860	ESO 143-G09	20 04 29	-61 14 42	1	SB(r)ab	4385	13.68	0.020
NGC 6890	MCG-07-41-023	20 14 49	-44 57 48	2	SB(r)ab	2459	12.82	0.008
NGC 7130	IC 5135	21 45 20	-35 11 07	2-SB	Sa pec	4850	12.88	0.000
NGC 7213	ESO 288-G43	22 06 08	-47 24 45	Lin-1	SA(s)0 <sup>0</sup>	1767	11.13	0.000
NGC 7582	ESO 291-G16	23 15 38	-42 38 36	2-SB	SB(s)ab	1551	10.83	0.000

**Table 1.** Column (5) gives the activity class of the galaxy, where SB means Starburst. Column (7) gives the radial velocity relative to the local group (in  $\text{km s}^{-1}$ ), while column (8) lists the total blue magnitude of the galaxies and column (9) contains the foreground galactic value of  $E(B-V)$  (extracted from the Nasa Extragalactic Database).

from the nuclei. There is no similar database with this quality for so many galaxies in the literature.

Fig. 1 shows representative spectra of four of the sample galaxies for several positions along the slit. Notice that absorption features are well detected in all spectra, as well as variations of spectral characteristics with distance from the nuclei. Signatures of young stellar populations, in particular, are clearly present in several of the spectra shown: over the whole inner 8'' of Mrk 732, more conspicuously at 4'' NE ( $r = -4''$  in Fig. 1); at  $\sim 8''$  from the nucleus in IC 1816, and at  $\sim 8$ – $12''$  in NGC 1097 (corresponding to the locus of the nuclear ring; Storchi-Bergmann, Wilson & Baldwin 1996). Further examples of the spatially resolved spectra are shown in Fig. 45.

### 3 METHOD OF ANALYSIS

Our main goal is to study the run of the stellar absorption features with distance from the nucleus. To this end, the analysis of each of the sample spectra consisted of (1) determining the ‘pseudo’-continuum in selected pivot-points (3780, 4020, 4510, 4630, 5313, 5870 and 6080 Å) and (2) measuring the equivalent widths of the CaII K and H, CN, G-band, MgI+MgH and NaI absorption lines integrating the flux with respect to the pseudo continuum.

The continuum and W measurements followed the method outlined by Bica & Alloin (1986a,b), Bica (1988) and Bica, Alloin & Schmitt (1994), and subsequently used in several studies of both normal and emission line galaxies (e.g., Bonatto, Bica & Alloin 1989, Storchi-Bergmann, Bica

LOG OF OBSERVATIONS								
NAME	DATE	EXP. TIME (sec)	PA [°]	AIR MASS	$\phi$ [°]	PIXEL	SCALE pc/arcsec	COMMENTS
Mrk 348	6/7 Dec. 94	1800	170	2.20	170	0.9	302	
3 C 33	6/7 Dec. 94	1800	65	1.43	167	0.9	1114	
NGC 526a	5/6 Dec. 94	3600	124	1.02	69	0.9	372	
Mrk 573	6/7 Dec. 94	1800	125	1.64	131	0.9	334	
IC 1816	6/7 Jan. 94	1800	90	1.07	82	1	328	
NGC 1097	6/7 Jan. 94	1800	139	1.01	88	1	77	
ESO 417-G6	6/7 Dec. 94	3600	155	1.01	69	0.9	310	
NGC 1326	5/6 Jan. 94	1800	77	1.15	88	1	80	
Mrk 607	6/7 Jan. 94	900	135	1.22	140	1	176	
NGC 1358	6/7 Jan. 94	900	145	1.23	136	1	257	
NGC 1386	6/7 Jan. 94	1800	169	1.12	89	1	48	
NGC 1433	6/7 Dec. 94	1200	19	1.05	19	0.9	59	
Pks 0349-27	5/6 Dec. 94	3600	82	1.04	103	0.9	1240	
NGC 1598	6/7 Jan. 94	1800	123	1.13	65	1	319	
NGC 1672	5/6 Jan. 94	1800	94	1.32	63	1	75	
CGCG 420-015	6/7 Jan. 94	900	40	1.46	140	1	570	
ESO 362-G8	6/7 Jan. 94	1800	165	1.17	88	1	298	
ESO 362-G18	6/7 Jan. 94	1800	55	1.19	82	1	233	
PICTOR A	6/7 Dec. 94	1800	71	1.15	71	0.9	666	
Pks 0634-20	5/6 Dec. 94	3600	139	1.07	129	0.9	1055	
Pks 0745-19	6/7 Dec. 94	1800	150	1.03	149	0.9	2323	
Mrk 1210	5/6 Jan. 94	1800	163	1.25	163	1	253	
NGC 2935	5/6 Jan. 94	1800	0	1.02	182	1	134	
NGC 3081	28/29 May 92	1200	73	1.25	70	0.9	140	seeing 3''
Mrk 732	6/7 Jan. 94	1800	55	1.50	31	1	560	
IRAS 11215-2806	5/6 Jan. 94	900	145	1.02	76	1	262	
MCG-05-27-013	6/7 Jan. 94	1800	0	1.20	78	1	470	
NGC 4303	28/29 May 92	1800	112	1.69	50	0.9	96	
MCG-02-33-034	6/7 Jan. 94	1800	25	1.24	55	1	284	
FAIRALL 316	6/7 Jan. 94	1800	100	1.29	102	1	308	
NGC 5135	29/30 May 92	1800	30	1.25	100	0.9	256	
NGC 5248	28/29 May 92	1800	146	1.58	144	0.9	73	
NGC 5643	28/29 May 92	1800	90	1.19	75	0.9	69	
NGC 6221	28/29 May 92	1800	5	1.24	56	0.9	88	clouds
NGC 6300	28/29 May 92	1800	124	1.19	18	0.9	63	clouds
NGC 6814	29/30 May 92	1800	161	1.06	170	0.9	108	clouds
IC 4889	28/29 May 92	1800	0	1.12	29	0.9	160	clouds
NGC 6860	28/29 May 92	1800	70	1.21	36	0.9	283	clouds
NGC 6890	29/30 May 92	1800	153	1.03	12	0.9	159	clouds
NGC 7130	29/30 May 92	900	143	1.01	50	0.9	314	
NGC 7213	29/30 May 92	1200	50	1.04	0	0.9	114	
NGC 7582	6/7 Jan. 94	300	67	1.53	83	1	100	

**Table 2.** Details of the observations. Column (4) lists the slit position angle (PA). The parallactic angle ( $\phi$ ) is listed in column (6). Column (7) lists the pixel size in arcsec, while column (8) lists the spatial scale in pc arcsec<sup>-1</sup>.

& Pastoriza 1990, Jablonka, Alloin & Bica 1990, Storch-Bergmann, Kinney & Challis 1995b, McQuade, Calzetti & Kinney 1995). This method consists of determining a pseudo-continuum in a few pivot-wavelengths and integrating the flux difference with respect to this continuum in pre-defined wavelength windows (Table 3) to determine the Ws. The pivot wavelengths used in this work are based on those used by the above authors and were chosen to avoid, inasmuch as possible, regions of strong emission or absorption features. The use of a compatible set of pivot points and wavelength windows is important because it will allow a detailed quantitative analysis of the stellar population—via synthesis techniques using Bica’s (1988) spectral library of star clusters—to be presented in a forthcoming paper. Here we will use our measurements only to look for broad

LINE WINDOWS	
CaII K	3908–3952
CaII H+He	3952–3988
CN	4150–4214
G band	4284–4318
MgI+MgH	5156–5196
NaI	5880–5914

**Table 3.** Wavelength windows used to measure the equivalent widths of the absorption lines.

trends in the properties of the stellar populations, and to identify signs of a nuclear FC (see below).

The determination of the continuum has to be done

**Figure 1.** Selected examples of the spatially resolved spectra of four of the sample galaxies. The nuclear spectra are indicated by thick lines. The angular distances from the nuclei are indicated, positive values corresponding to West (W, NW or SW) or South direction (in the case when the observed PA is  $0^\circ$ ). The spectra are normalized at 5870 Å and shifted vertically by one unit to facilitate comparison. Residual sky emission lines have been ticked out.

interactively, taking into account the flux level, the noise and minor wavelength calibration uncertainties as well as anomalies due to the presence of emission lines. The 5870 and 6080 Å points, in particular, are sometimes buried underneath HeI 5876 and [Fe VII]6087 Å emission lines (for instance, in the nuclear regions of IC 1816, Mrk 348 and NGC 3081). In such cases the placement of the continuum was guided by adjacent wavelength regions. In a few cases,

it was also necessary to make ‘cosmetic’ corrections when a noise spike was present in the wavelength window used to compute the W. We emphasize, however, that such anomalies were very rare. In the majority ( $> 90\%$ ) of cases the excellent quality of the spectra allowed a precise determination of the continua and Ws.

Fig. 2 illustrates the application of the method to four of the sample spectra. The spectrum in Fig. 2a corresponds

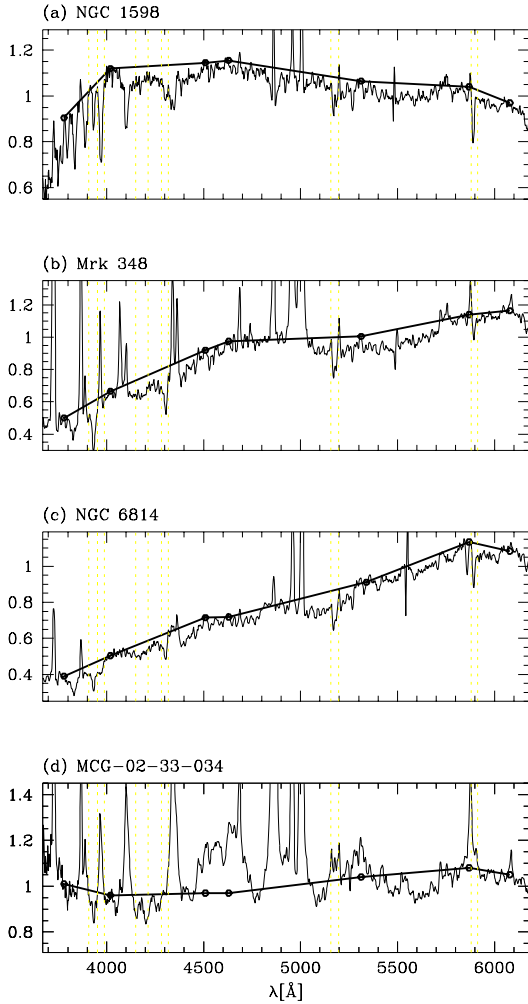


**Figure 2.** Illustration of the continuum determination procedure for the nuclear spectra of the LINER NGC 1598 (a), the Seyfert 2 Mrk 348 (b), and the Seyfert 1 galaxies NGC 6814 (c) and MCG -02-33-034 (d). The continuum pivot points are marked by the filled circles. Dashed vertical lines indicate the wavelength windows used to measure the equivalent widths of Ca K and H, CN, G band, Mg and Na lines.

to the nucleus of the LINER NGC 1598. The spectrum is almost purely stellar, posing no difficulties to the determination of the pseudo continuum. Note that the continuum runs well above the actual spectrum except in the pivot points. Fig. 2b shows the nuclear spectrum of Mrk 348, a type 2 Seyfert. Here, as for all Seyfert 2s in the sample, the continuum can still be placed with little ambiguity, despite the presence of many emission lines. As in many other cases, the Ca H line is filled with [NeIII] and H $\epsilon$  emission in the central regions, but not in outer positions, an effect which must be taken into account when interpreting  $W(\text{Ca H})$  spatial gradients. Note also that, as in Fig. 2d, the 5870 and 6080 Å points are underneath HeI and [Fe VII] emission, respectively. This is not a problem, as the continuum can still be determined from the adjacent regions.

Whilst for most LINERs, Seyfert 2s and normal galaxies the placement of the continuum is straightforward, this is not the case in the nuclear regions of strong Seyfert 1s, where

the numerous broad lines and intense non-stellar continuum complicate the analysis. This is illustrated in Fig. 2d, where we plot the nuclear spectrum of MCG -02-33-034. The 4510, 4630 and 5313 Å points, in particular, are all underneath Fe II blends, making it impossible to determine them accurately. None of the absorption lines in Fig. 2d, with the possible exception of Ca K is free of contamination. The Mg line, for instance, is filled up by FeII and [NI]5200 Å emission, while the Na window is contaminated by broad HeI 5876 Å. It is clear that in extreme cases like this no reliable value for the  $W$ s of the absorption lines can be derived with our or any other method. The presence of such a strong nuclear FC should appear as a dip at  $r = 0$  in the radial profiles of the  $W$ s, and this is indeed seen in Fig. 7. However, given the difficulties in defining a continuum, the depth of this dip is unreliable. At any rate, the only other galaxy in the present sample with a spectrum as complex as MCG -02-33-034 is the Broad Line Radio Galaxy Pictor A (Fig. 32). For less extreme Seyfert 1s like NGC 6814 (Fig. 2c), the continuum can be defined with little ambiguity.

The four examples in Fig. 2 span essentially all types of spectra found in the sample. Overall, we found that the method works well for most spectra, with the exception of the nuclear regions of strong Seyfert 1s. The comparison of the  $W$ s and continuum colors in the nuclear and outer regions is a useful tool to detect the presence of a FC, particularly in Seyfert 2s and LINERs, where the FC, if present, is not as conspicuous as in type 1 objects. Indeed, one of our major goals is to verify whether Seyfert 2s and LINERs exhibit signs of such a nuclear FC, which should cause a dilution of the absorption lines with respect to those measured outside the nucleus.

### 3.1 Consistency and Error Analysis

The positioning of the continuum can be somewhat subjective, particularly in the noisier spectra, given that it has to be carried out interactively. In order to verify whether our measurements are consistent with those of Bica (1988) we have measured the continuum fluxes and  $W$ s of the 15 templates corresponding to his spectral groups E1–E8 and S1–S7. The difference between his and our continuum measurements is of the order of 1%. For the  $W$ s the difference is typically  $\approx 0.5$  Å and always smaller than 1 Å, corresponding to an agreement at a 5–10% level. This compatibility is important, since it insures that we can apply stellar population characterization techniques similar to those employed by Bica.

In the discussion of our results (Section 4) we will compare the  $W$ s and continua of the galaxies in the present sample with templates S1 to S7 and E1 to E8 of Bica (1988) as a guide to obtain a broad characterization of the stellar populations. (As pointed out in the previous section, a full quantitative analysis of the stellar populations will be presented in a forthcoming paper.) These templates correspond to increasing contributions of young components, from S1 and E1, to S7 and E8. Templates S1 to S3 and E1 to E6 are composed of old ( $> 5 \times 10^9$  yr) and intermediate age stars ( $5 \times 10^8$ – $10^9$  yr), differing mostly on the contribution from stars of different metallicities. From S4 to S7 and E7 to E8 we have an increasing contribution from young stars ( $< 10^8$

yr), which can reach as much as 65% for S7 and 20% for E8 of the flux at 5870 Å.

The Ws measured in this work are subjected to two different sources of error: (1) the noise present in the spectra, and (2) the uncertainty in the placement of the continuum.

The error in the Ws due to noise was evaluated using standard propagation of errors. The noise level was computed from the rms dispersion in a 60–100 Å region free of strong emission or absorption lines. Two windows, one in the 4200 Å region and the other around 5650 Å, were used for this purpose. The noise in the first window was used to compute the errors in the Ws of Ca K and H, CN and G-band, whereas the latter window was used for the Mg and Na lines. The resulting errors are typically 0.5 Å for the ‘blue’ lines (Ca K to G-band), and 0.3 Å for Mg and Na. The errors in the central regions are usually smaller than these average values, since the noise is lower there. The Ca K line in NGC 7213, for instance, has an error of  $\sim 0.3$  Å in the central 5'', gradually increasing to  $\sim 0.7$  Å for  $r > 22''$ .

The uncertainties in the placement of the continuum are less straightforward to evaluate, since, as explained above, the continuum is not automatically defined, but determined interactively. To compute the error in the Ws associated with this source of uncertainty we have re-analyzed the spectra of 4 galaxies (42 extractions in total), defining upper and lower values of the continuum at the pivot-points. The mean difference between these values and the adopted one (all evaluated in the middle of the line-window), was taken as a measure of the error in the continuum flux, which was then propagated to the Ws. We found that the resulting errors are typically 30–50% larger than the errors due to noise alone. As expected, the uncertainty in the positioning of the continuum increases with decreasing S/N. Since it is not practical to measure lower and upper continua for all 491 spectra, we have used this scaling between the S/N ratio and the continuum errors measured above to estimate the errors due to the positioning of the continuum for the remaining objects.

The combined error in the Ws due to noise and continuum positioning, added in quadrature, are typically 0.5 Å for Ca K, Ca H and the G-band, 0.4 Å in Mg and Na, and 1.0 Å for the CN line. The larger error in the CN reflects the fact that this feature is very shallow, being essentially a measure of the local height of the pseudo continuum above the actual spectrum. In fact, it is often difficult to identify the CN feature in the spectra (e.g., Fig. 2). Indeed, the CN band is only pronounced in very metal rich populations, such as templates S1 and E1 of Bica (1988). We nevertheless keep this line in our analysis, since our measured Ws are consistent with those found by Bica and in most cases its radial variations follow those of the other absorption lines.

In the discussion of our results, we shall put more emphasis on the Ca K, G-band and Mg features, since the Ca H line is often contaminated by emission and the CN line is subjected to larger errors. The Na line is not a good diagnostic of stellar population since it is partially produced in the interstellar medium of the host galaxy. This line can, however, be used as an indication of the presence of dust (Bica & Alloin 1986, Bica et al. 1991). In the attribution of template types to the different spectra a larger weight is given to Ca K, since this is often the strongest line, less affected by errors. As discussed in section 4.1, sometimes

different lines indicate different template types, which simply indicates a different mixture of stellar populations than found in Bica’s (1988) grid of spectral templates.

The uncertainty in the determination of the Ws limits the degree of dilution measurable from our data. The effect of a FC contributing a fraction  $f_{FC}$  of the total flux in a given wavelength is to decrease the W of an absorption line in this wavelength by this same factor:  $\Delta W = f_{FC} W$ . Therefore, the minimum amount of dilution that can be safely measured from the radial variations of a line with an W of, say, 10 Å and an error of 0.5 Å is  $\sim 5\%$ . From the results presented in the next section we estimate that this method of evaluating the contribution of a FC works well for  $f_{FC} \gtrsim 10\%$  for the present data set as a whole, though smaller lower limits are reached in the best spectra.

## 4 RESULTS

The main results of the data analysis are presented in Figs. 3–44, where we plot the radial variations of the Ws, colors and surface brightness for all the galaxies in the sample. The upper panel shows the Ws of Ca K (solid line) and Ca H (dashed) against the distance from the nucleus ( $r$ ). Similarly, the second panel shows the Ws of the G-band (solid) and CN (dashed), while the third panel shows Mg (solid) and Na (dashed). Negative values of the W indicate emission, as often found in the Ca H plots due to contamination by [NeIII] and H $\epsilon$ . The Mg and Na lines are also contaminated by emission in some cases. Apart from such cases (discussed in detail in Section 4.1), a dip in the W plots indicates dilution of the absorption lines by a FC or the presence of a young stellar population. The fourth panel shows the color profiles, mapped by the ratios of the 5870 to 4020 Å (solid line) and 4630 to 3780 Å (dashed line) pseudo-continuum fluxes. (Note that the left hand scale in this plot corresponds to  $F_{5870}/F_{4020}$ , whereas the values in right correspond to  $F_{4630}/F_{3780}$ .) Dips in the color plots indicate a blue continuum, whereas peaks indicate a red continuum, due to an old stellar population and/or reddening. The colors have been corrected by foreground galactic reddening using the values of E(B–V) in Table 1. This correction, besides being small, does not affect the shape of the curves. Finally, to give a measure of the flux level in each position the bottom panels show the run of the surface brightness in the 5870 Å pseudo continuum with distance from the nucleus.

In order to better illustrate the results presented in Figs. 3–44, Fig. 45 shows the spatially resolved spectra of five galaxies, representing the five classes of objects studied, zoomed into the wavelength regions of the absorption lines analysed in this work. This figure also serves as a further illustration of the determination of the pseudo-continuum and of the quality of the current database.

We start our discussion of the results with the cases of NGC 1097, NGC 1433 and NGC 1672. The presence of star-forming rings in these galaxies serves as a good illustration of the consistency of our measurements and as a guide to the interpretation of the W and color gradients in other objects. NGC 1326, 2935, 4303 and 5248 also present star-forming rings, and much of the the discussion below also applies to these objects.

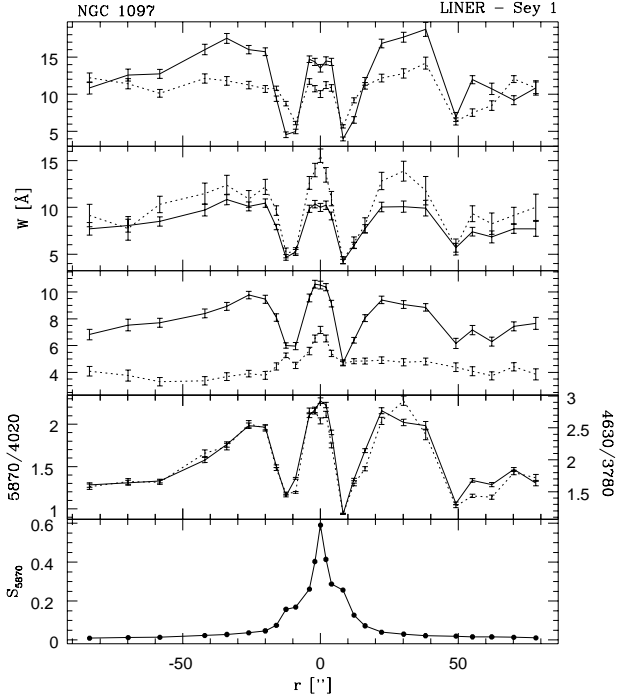


**Figure 3.** Radial variations of the equivalent widths (W), colors and ‘surface brightness’ for NGC 1097. The upper panel plots the Ws of CaII K (solid line) and CaII H (dashed), while the second panel shows G-band (solid), CN (dashed), and the third shows MgI+MgH (solid) and NaI (dashed). The fourth panel shows the radial variations of the continuum colors, mapped with the  $F_{5870}/F_{4020}$  (solid line, left hand scale) and  $F_{4630}/F_{3780}$  (dashed line, right hand scale) flux ratios. Red is up and blue is down in this plot. The bottom panel shows the run of the surface brightness at 5870 Å (in units of  $\text{erg cm}^{-2} \text{s}^{-1} \text{Å}^{-1} \text{per arcsec}^2$ ) along the slit.

NGC 1097, a nearby spiral galaxy, has a low luminosity nucleus, characterized by a LINER like emission line spectrum, surrounded by a ring of HII regions (Sersic & Pastoriza 1965, 1967, Phillips et al. 1984). In addition to its LINER spectrum, the broad, double peaked, variable Balmer lines in the nucleus of NGC 1097 are a clear signature of the presence of an active nucleus in this galaxy (Storchi-Bergmann, Baldwin & Wilson 1993; Fig. 1). The low Ws and blue colors typical of the young stellar populations of the ring are remarkably well depicted in Fig. 3 by the dips at  $|r| \sim 10''$  in the radial profiles of the Ws and colors. Despite its active nucleus, the optical continuum shows little evidence of a blue featureless continuum of the kind found in type 1 Seyferts and QSOs. This is seen in Fig. 3, which shows that the Ws in the nucleus of NGC 1097 are not significantly diluted with respect to their values inside or outside the ring. On the contrary, the CN and Mg lines seem to be stronger in the nucleus than outside it, while the Na line clearly peaks at  $r = 0$ . The Ca K and H lines, however, do present a central dip, albeit of a low amplitude. Comparing the nuclear spectrum with the  $r = -4$  and  $+4''$  extractions we find variations of 7 and 11% in the Ws of Ca K and H respectively (§5.2), which indicates that an AGN continuum, if present, contributes less than  $\sim 10\%$  of the light in this wavelength region. Considering that the error in these Ws is  $\sim 5\%$ , the evidence for a diluting FC in NGC 1097 is marginal.

The Ws in NGC 1097 can be represented by a S2–S3 template at the nucleus, S6–S7 at the ring and S3 outwards. The continuum ratios are consistent with the spectral templates inferred from the Ws, with the exception of the nuclear region, where the continuum is redder, more typical of a S1 template. This could be interpreted as evidence of reddening of the nuclear regions, as is also indicated by the increase of  $W(\text{Na})$  towards the nucleus (Storchi-Bergmann et al. 1995a). This difference in template types can be accounted for with  $E(B - V) \approx 0.15$ . Storchi-Bergmann, Kinney & Challis (1995b) obtained a large aperture spectrum of this object ( $10'' \times 20''$ ), including the nucleus and part of the star-forming ring. Their measured Ws can be represented by a S5 template, which is comparable to our results in the inner  $10''$ . The IUE spectrum of NGC1097 is dominated by the ring, showing several absorption lines typical of young stars (Kinney et al. 1993).

NGC 1433 has been classified as a Seyfert 2 by Véron-Cetty & Véron (1986), though our spectrum presents emission line ratios more typical of LINERs. It also contains a star-forming ring  $\sim 8''$  from its nucleus (Buta 1986). As in the case of NGC 1097, the ring leaves a clear finger print in the W and color profiles (Fig. 36). No dilution of the absorption lines or blueing of the continuum is seen in the nuclear spectrum. Both the Ws and continuum ratios indicate similar spectral templates: S3 at the nucleus, S5 at the ring and S3 outwards. As in NGC 1097, the general decrease of the Ws and bluer colors towards large distances seen in Fig. 36 correspond to the stellar population of the disk of the galaxy.

NGC 1672 is a Sersic-Pastoriza galaxy, whose nucleus has already been classified as Starburst (Garcia-Vargas et al. 1990, Kinney et al. 1993), Seyfert 2 (Mouri et al. 1989) and LINER (Díaz 1985, Storchi-Bergmann et al. 1996b). Our nuclear spectrum is consistent with a LINER classification. Its W and color profiles (Fig. 38) are very similar to those of the previous two galaxies. Both Ws and continuum ratios indicate a S4 template at the nucleus, S7 at the  $r = 5''$  ring, S4 outside the ring, decreasing to values typical of S7 template in the outer regions.

The spatio-spectral variations in NGC 1672 are also seen in Fig. 45a. The correspondence between Figs. 38 and 45a is clear. The star forming ring, with its shallower absorption lines and bluer continuum, is visible in the  $r = -8$ ,  $+4$  and  $+8''$  extractions plotted in Fig. 45a. The blueing of the spectra towards the outer regions of the galaxy is also illustrated. The  $+67''$  extraction, in particular, crosses an HII region.

These three examples demonstrate that the method employed in this study is able to detect variations of the stellar populations as a function of distance to the nucleus. Star-forming rings, in particular, leave unambiguous signatures in the W and color profiles.

Since ‘dilution’ of the metal lines by a young stellar population is detectable, we also expect to be able to measure dilution by an AGN continuum. This is best illustrated in the case of Seyfert 1 objects, such as MCG-02-33-034 (Fig. 7), ESO 362-G18 (Fig. 5), NGC 6860 (Fig. 9), NGC 6814 (Fig. 8), and the Broad Line Radio Galaxy Pictor A (Fig. 32).

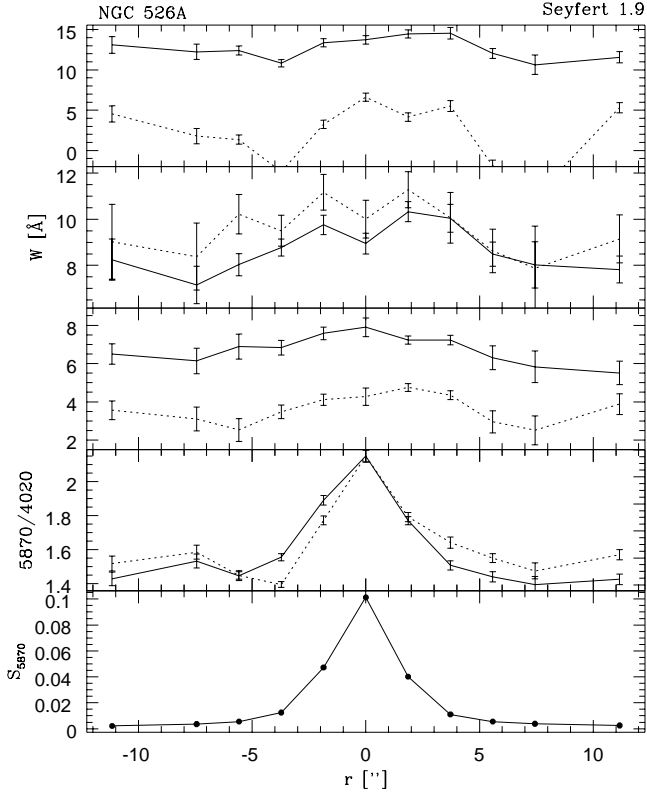


Figure 4. Same as Fig. 3.

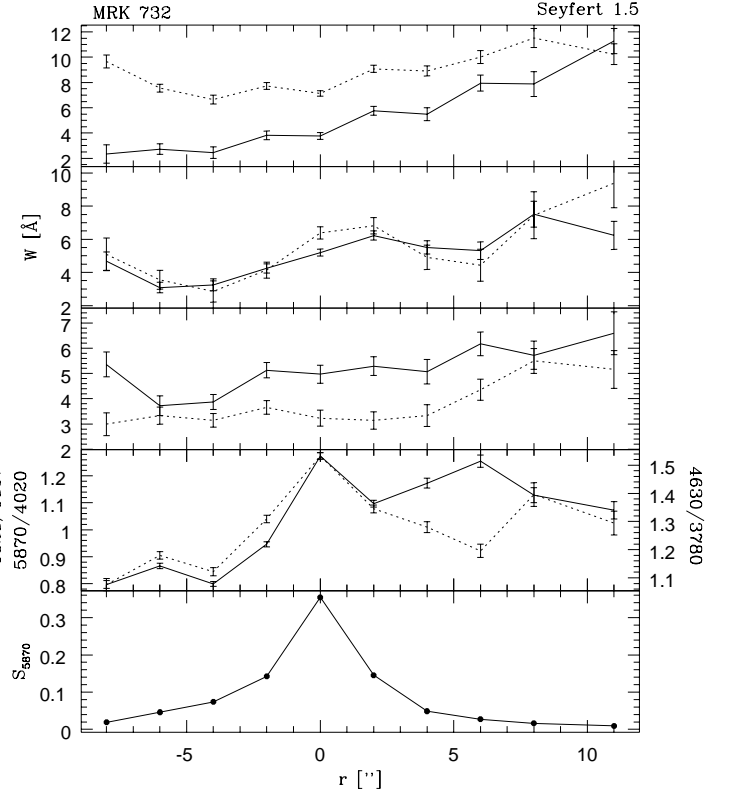


Figure 6. Same as Fig. 3.

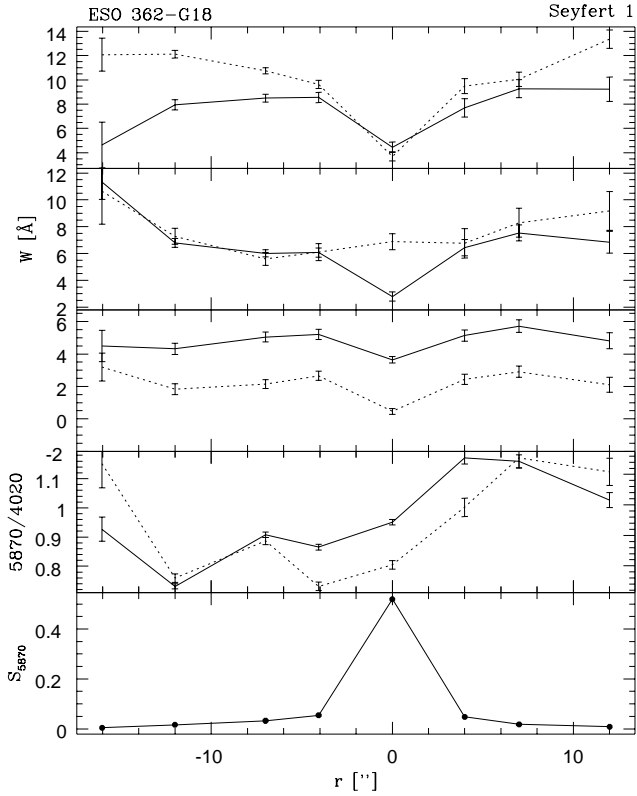


Figure 5. Same as Fig. 3.

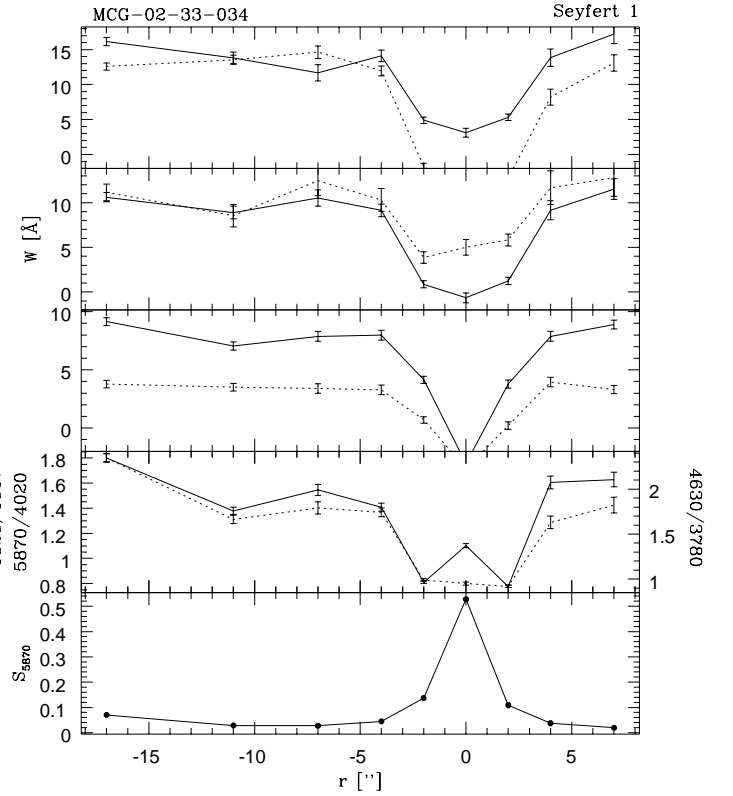


Figure 7. Same as Fig. 3.

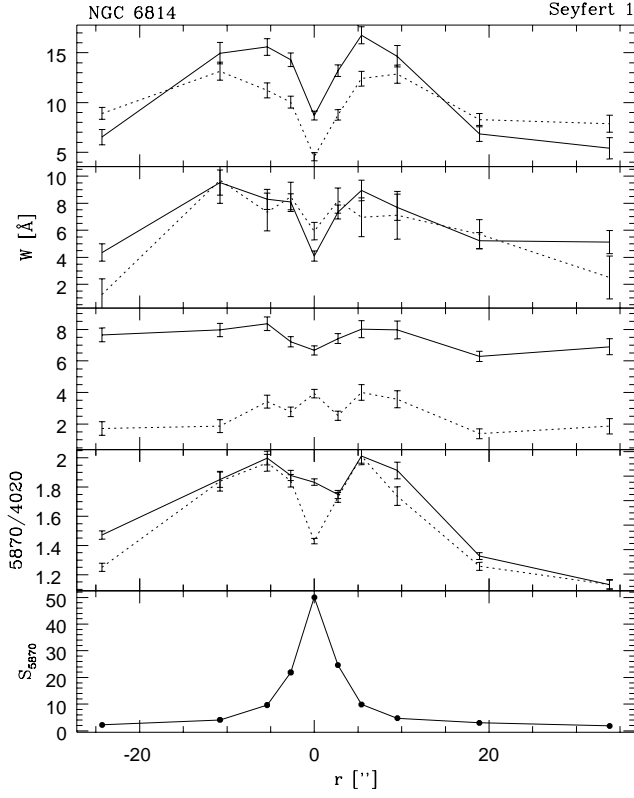


Figure 8. Same as Fig. 3.

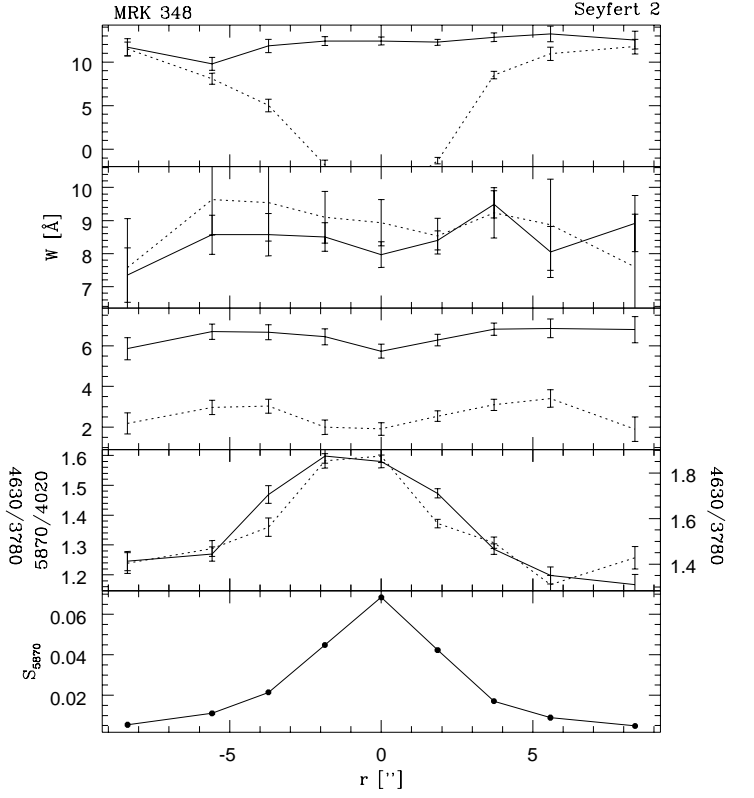


Figure 10. Same as Fig. 3.

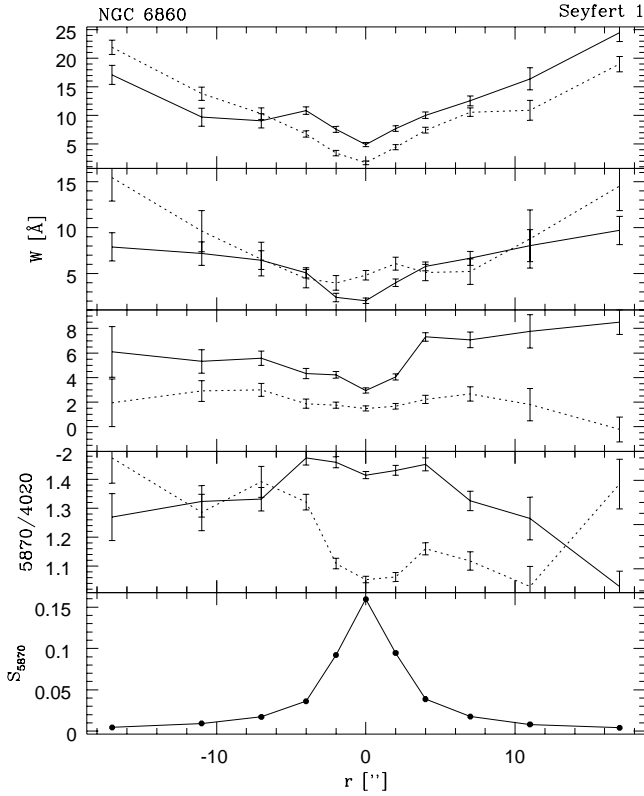


Figure 9. Same as Fig. 3.

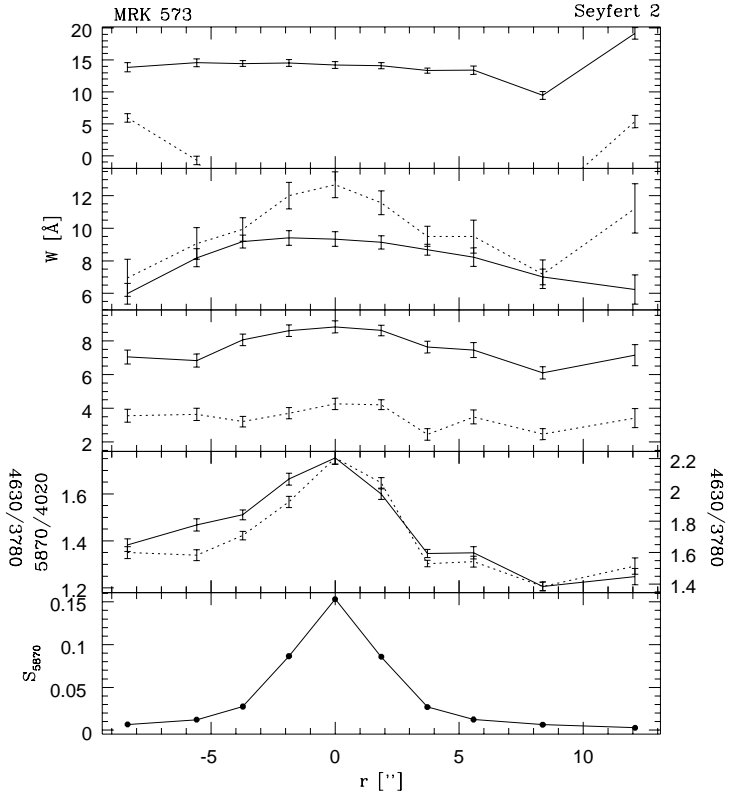


Figure 11. Same as Fig. 3.

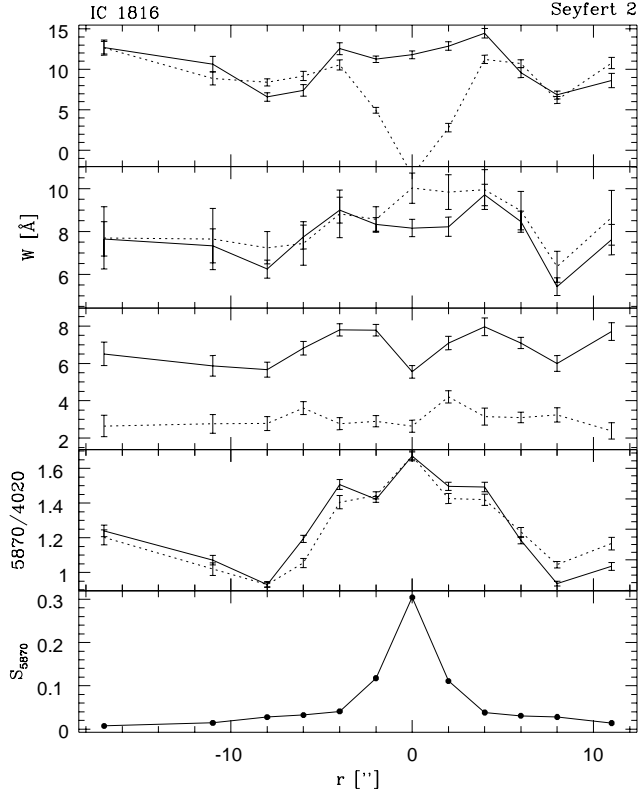


Figure 12. Same as Fig. 3.

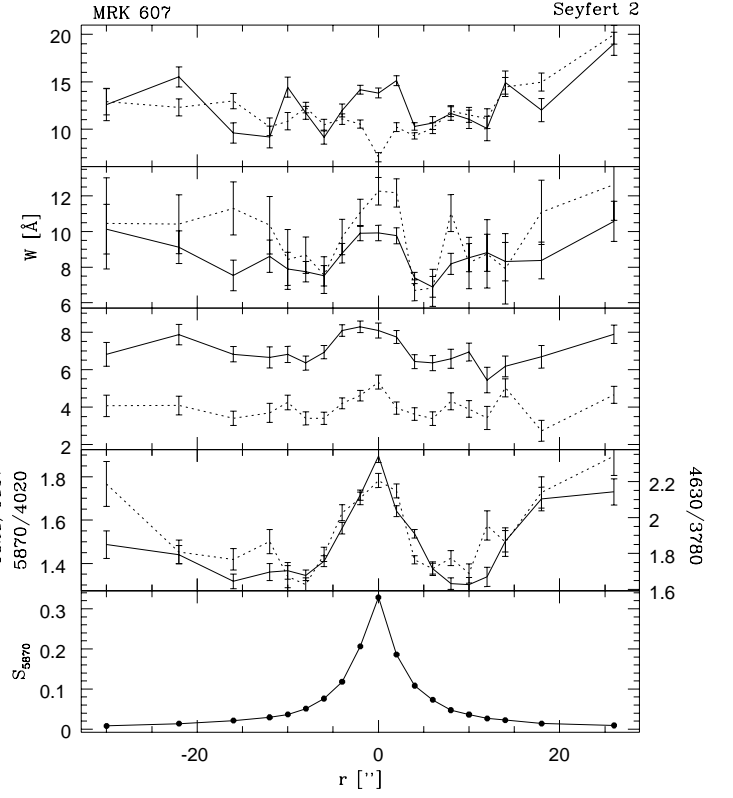


Figure 14. Same as Fig. 3.

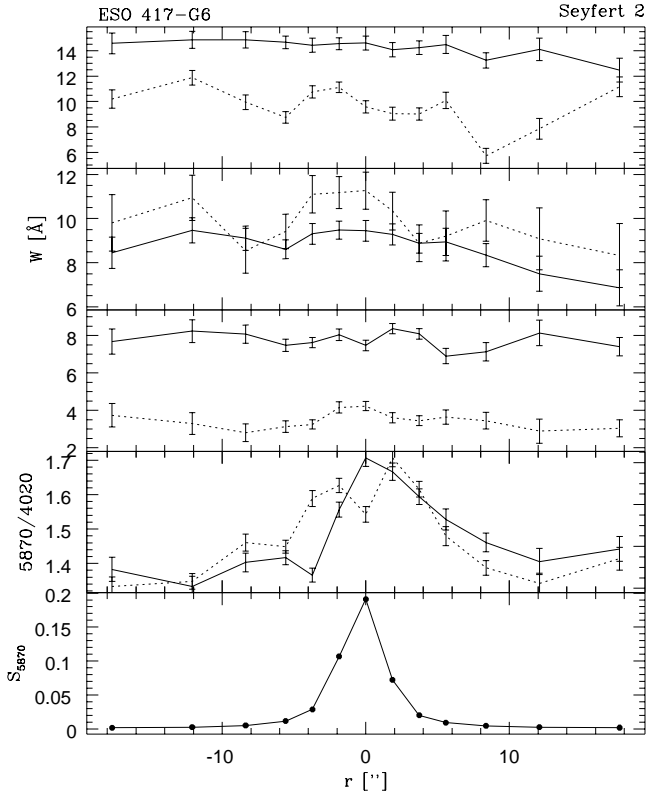


Figure 13. Same as Fig. 3.

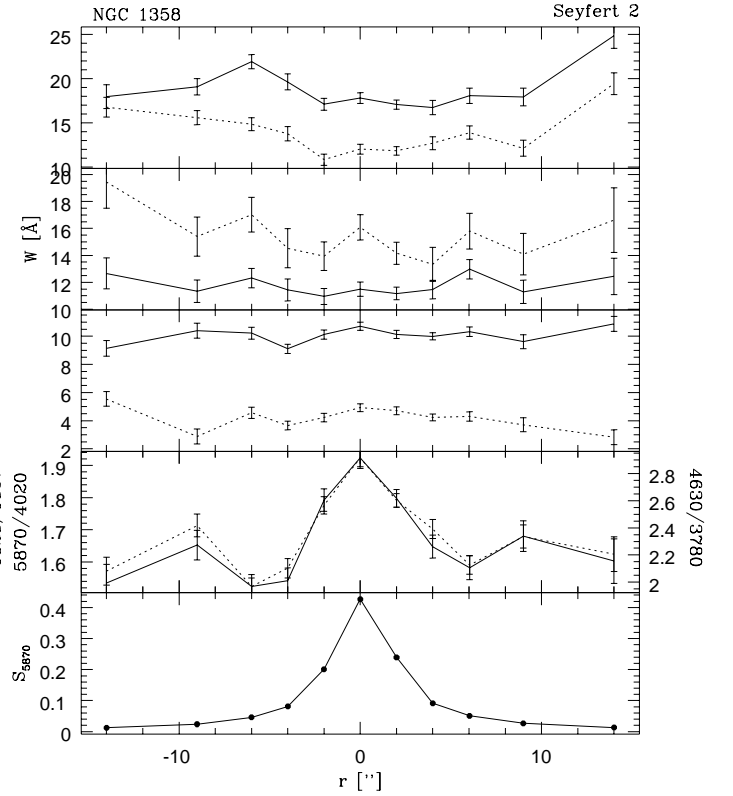


Figure 15. Same as Fig. 3.

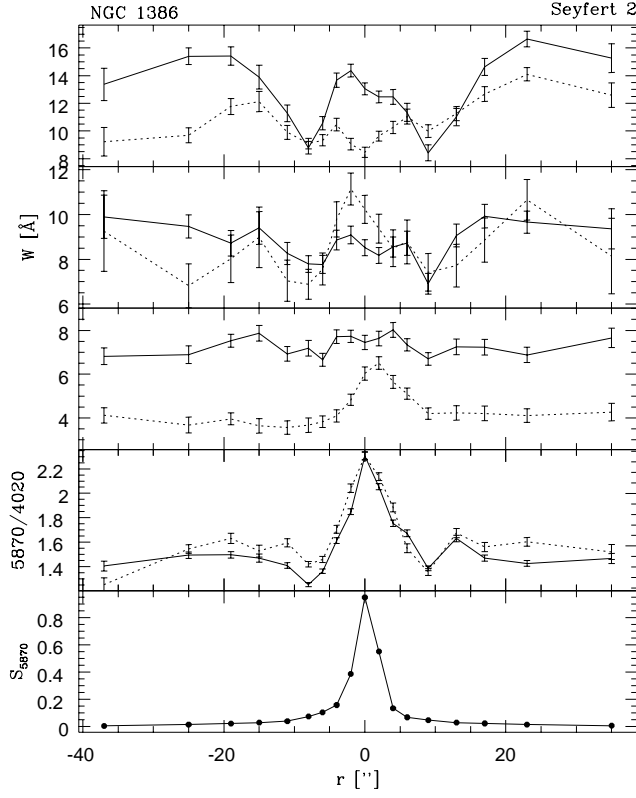


Figure 16. Same as Fig. 3.

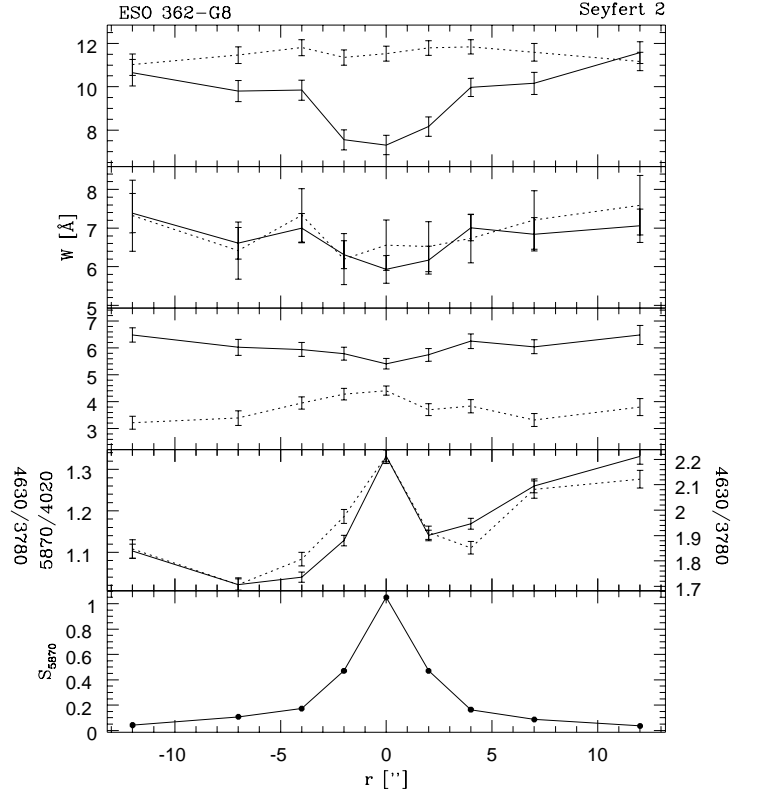


Figure 18. Same as Fig. 3.

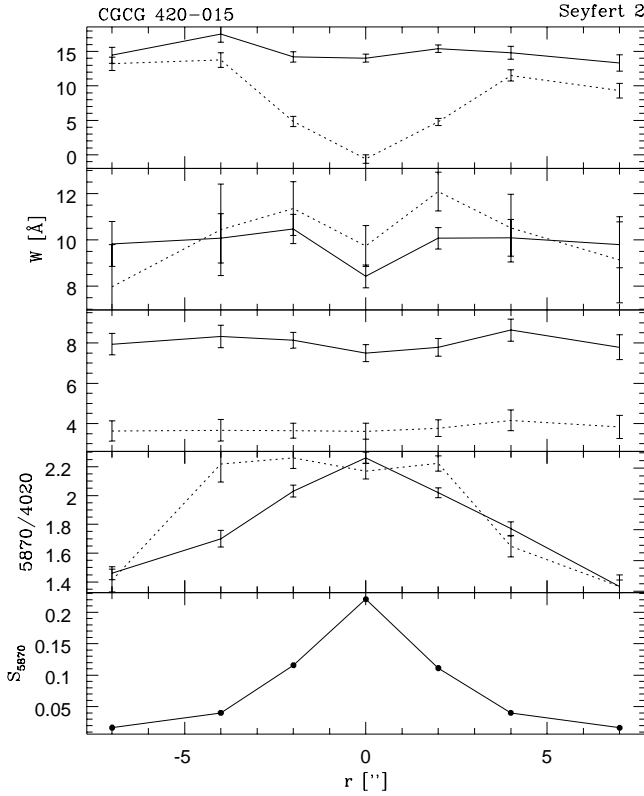


Figure 17. Same as Fig. 3.

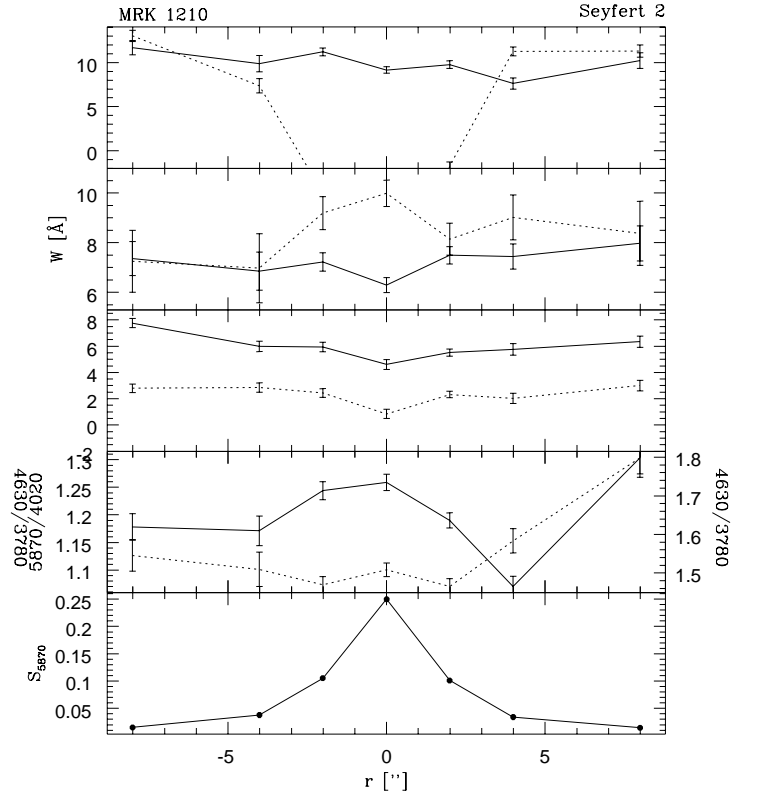


Figure 19. Same as Fig. 3.

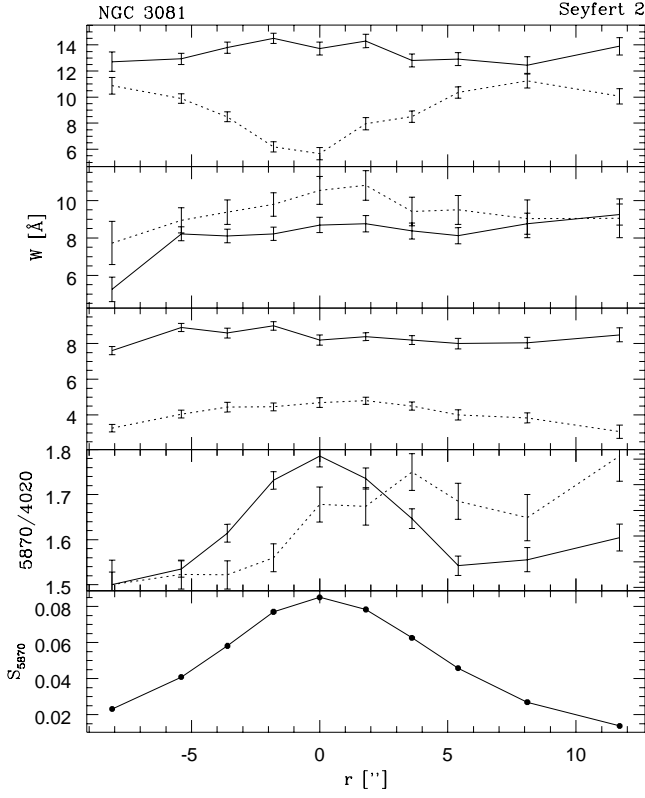


Figure 20. Same as Fig. 3.

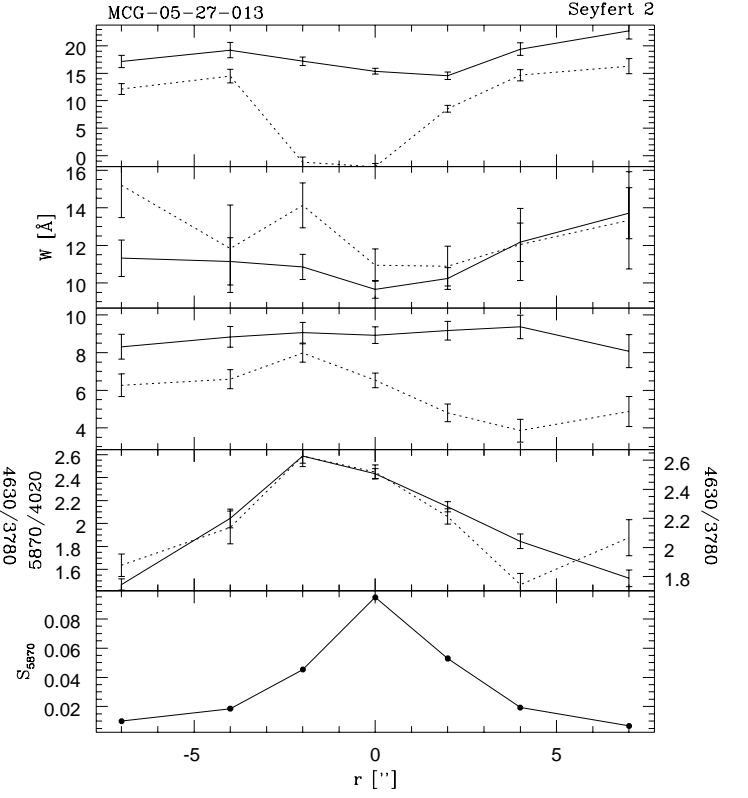


Figure 22. Same as Fig. 3.

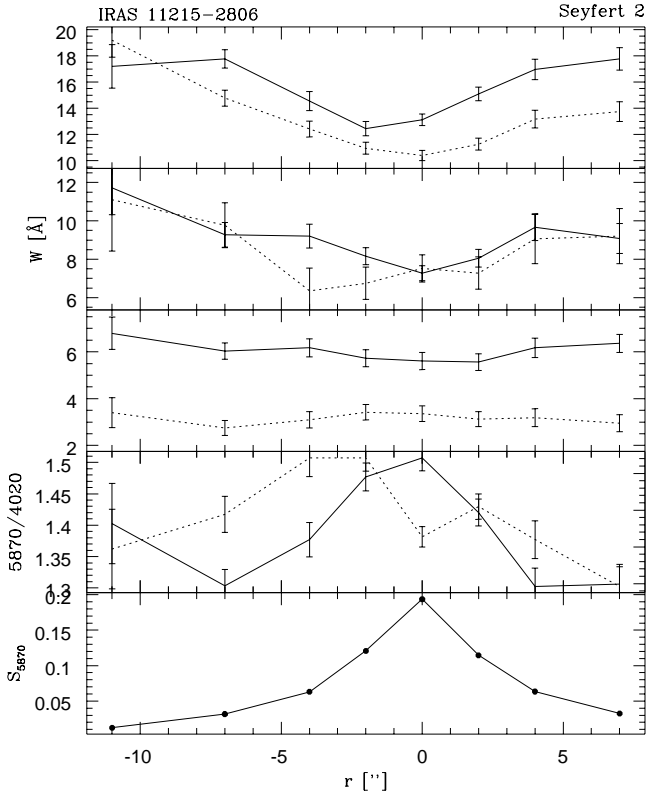


Figure 21. Same as Fig. 3.

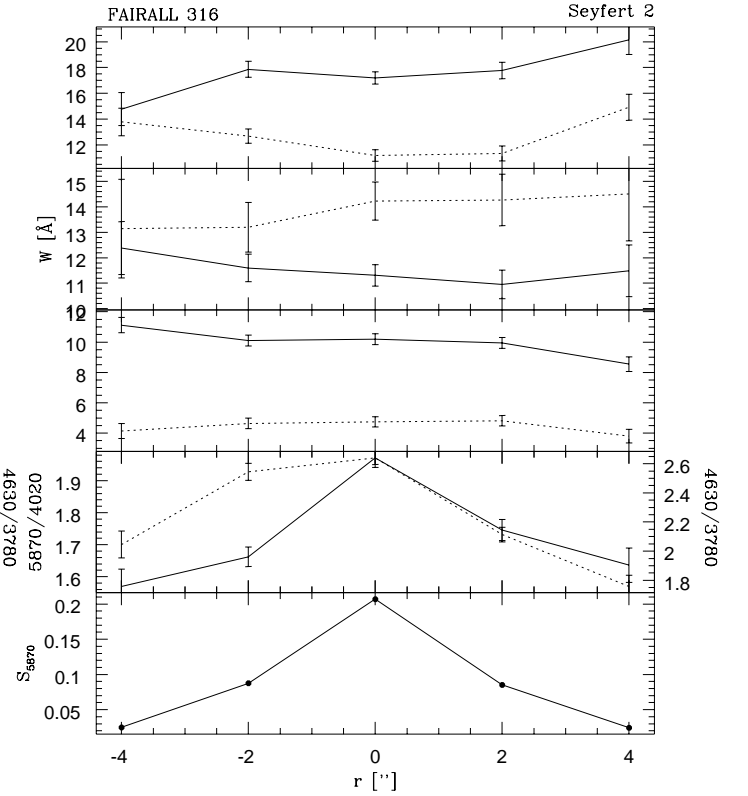


Figure 23. Same as Fig. 3.

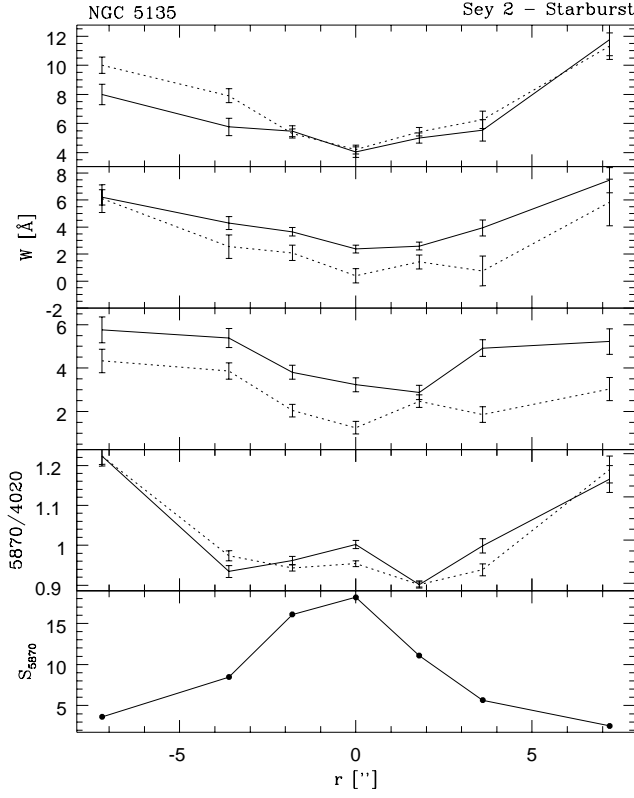


Figure 24. Same as Fig. 3.

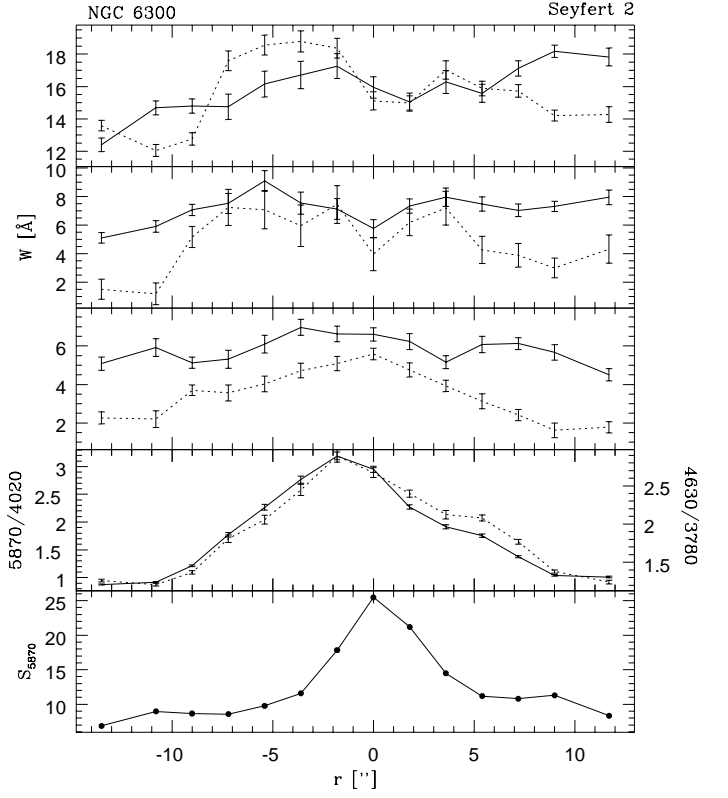


Figure 26. Same as Fig. 3.

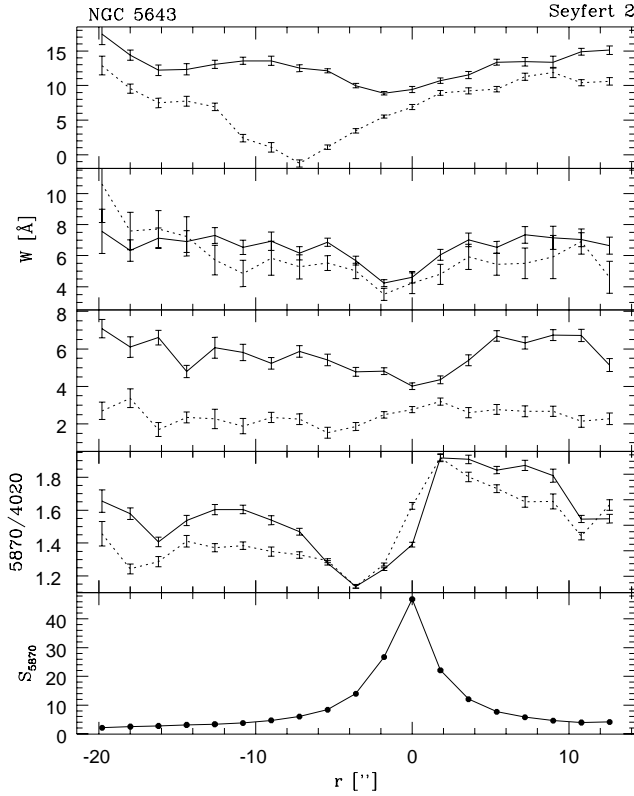


Figure 25. Same as Fig. 3.

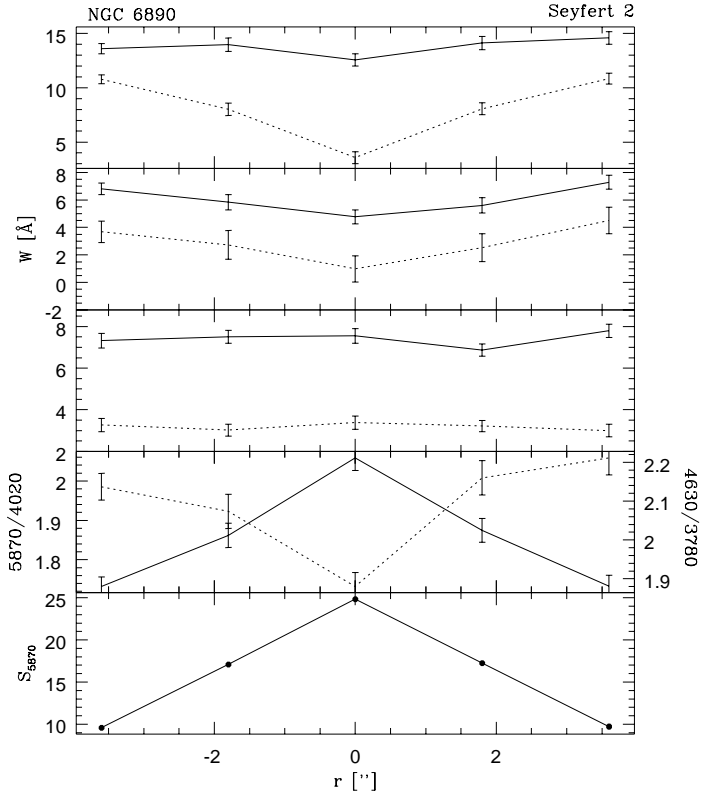


Figure 27. Same as Fig. 3.

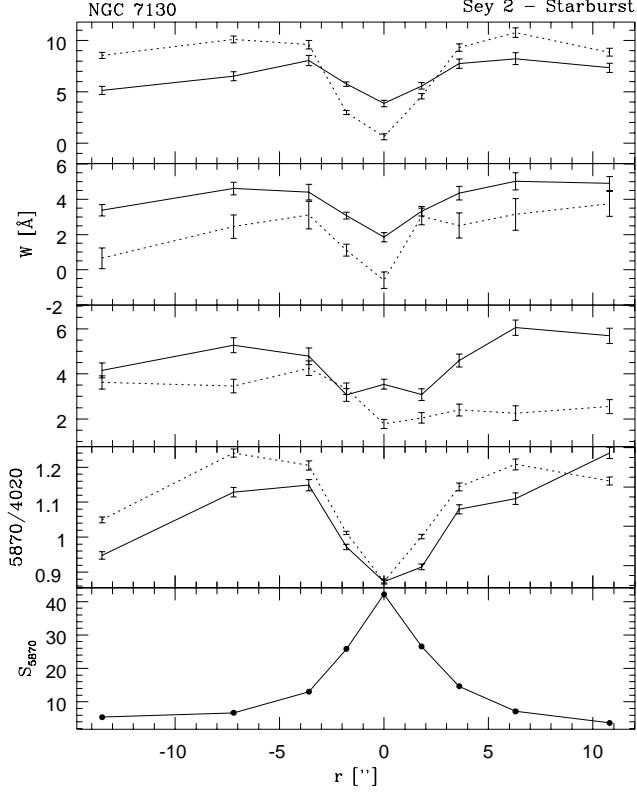


Figure 28. Same as Fig. 3.

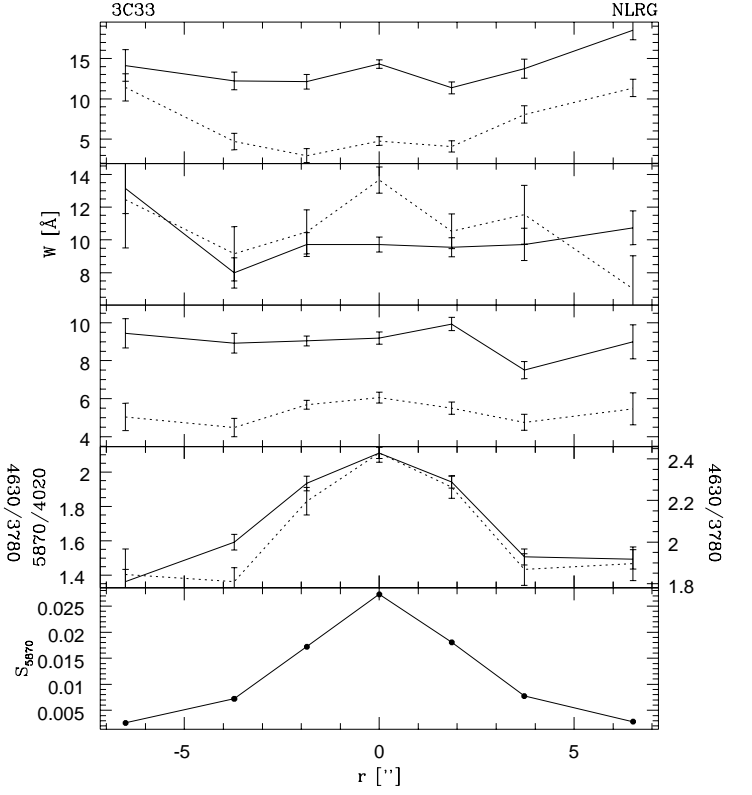


Figure 30. Same as Fig. 3.

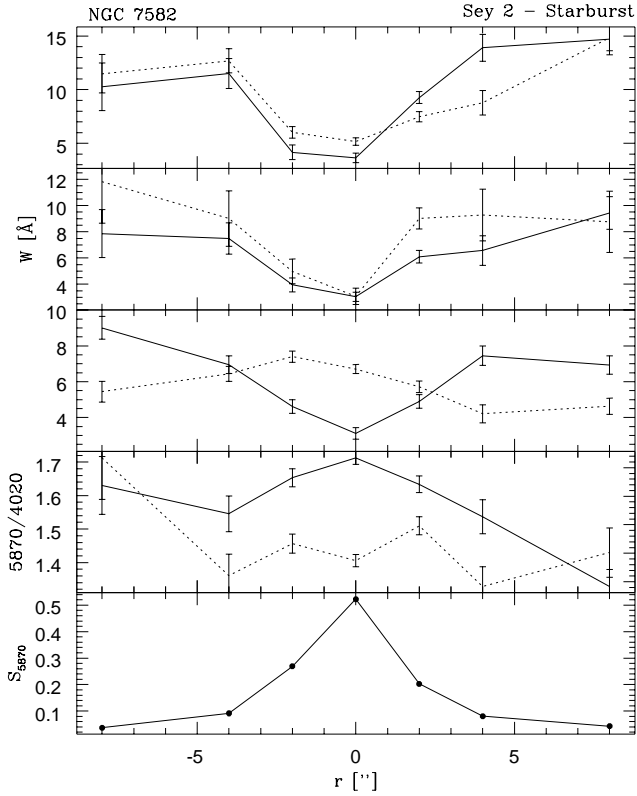


Figure 29. Same as Fig. 3.

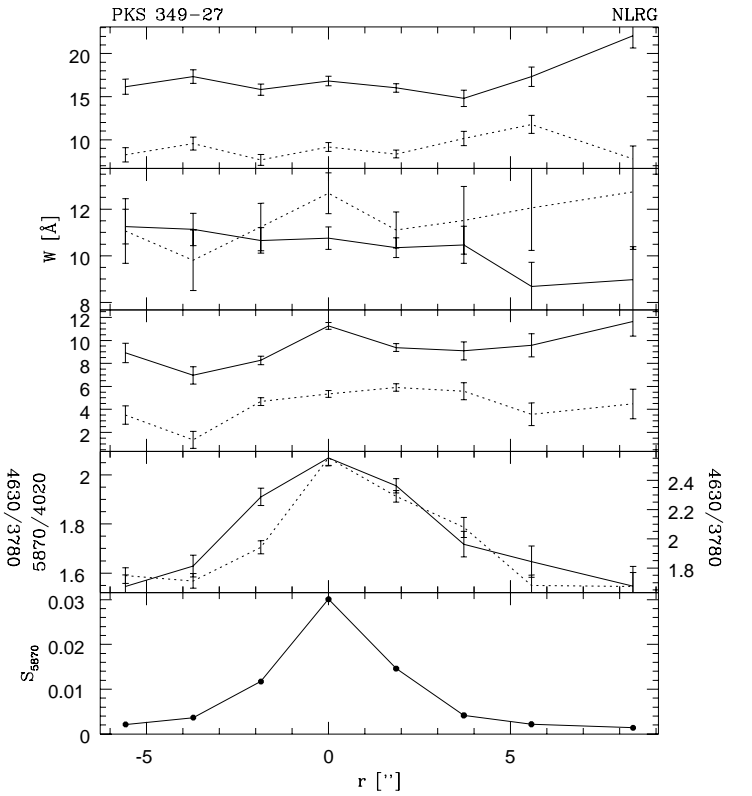


Figure 31. Same as Fig. 3.

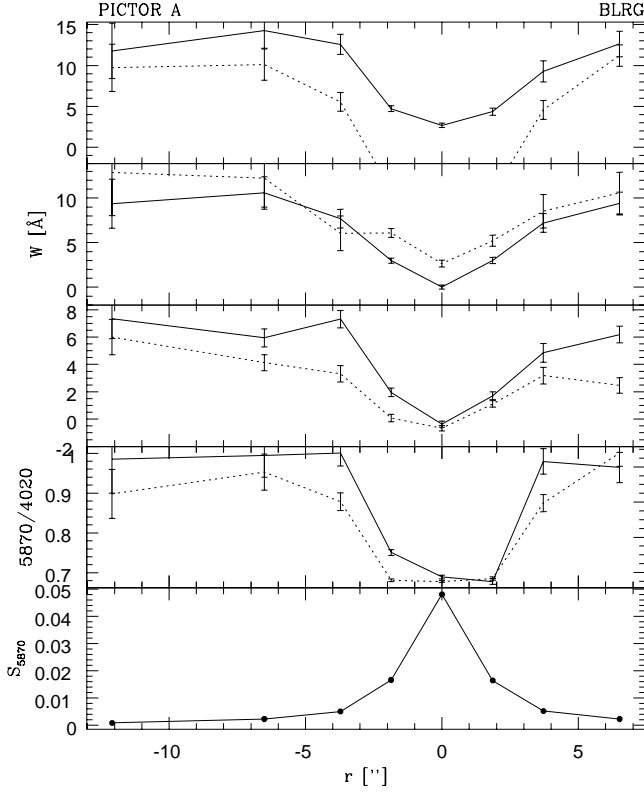


Figure 32. Same as Fig. 3.

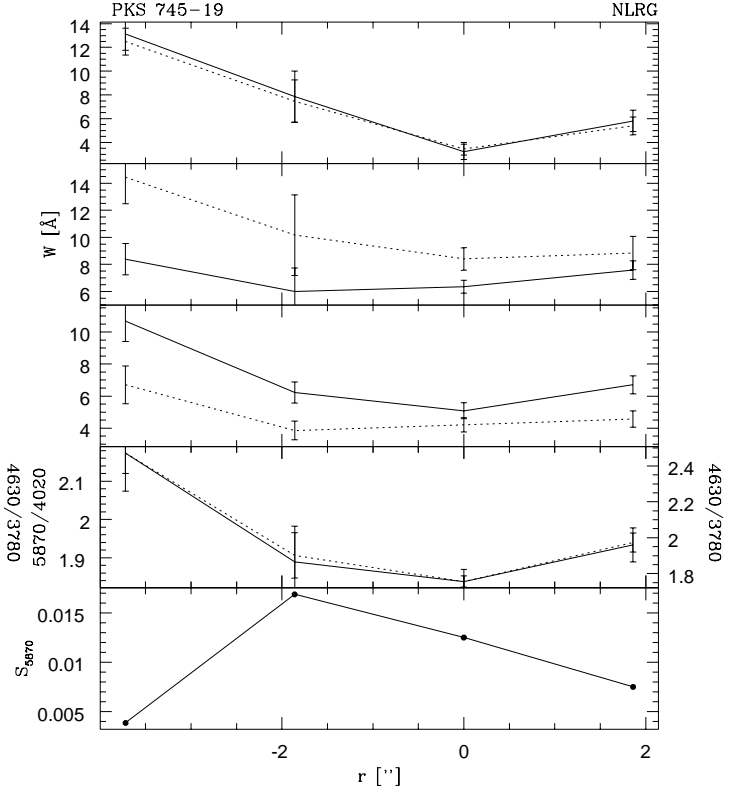


Figure 34. Same as Fig. 3.

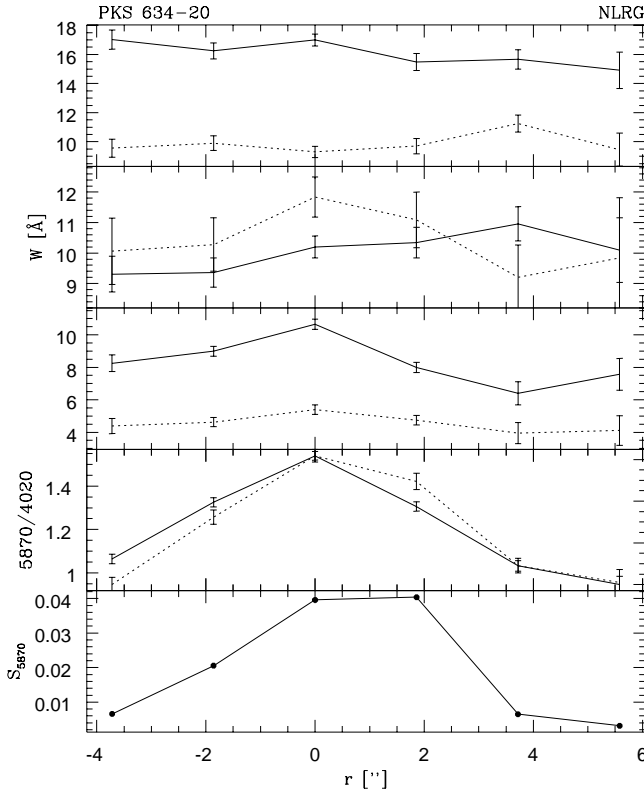


Figure 33. Same as Fig. 3.

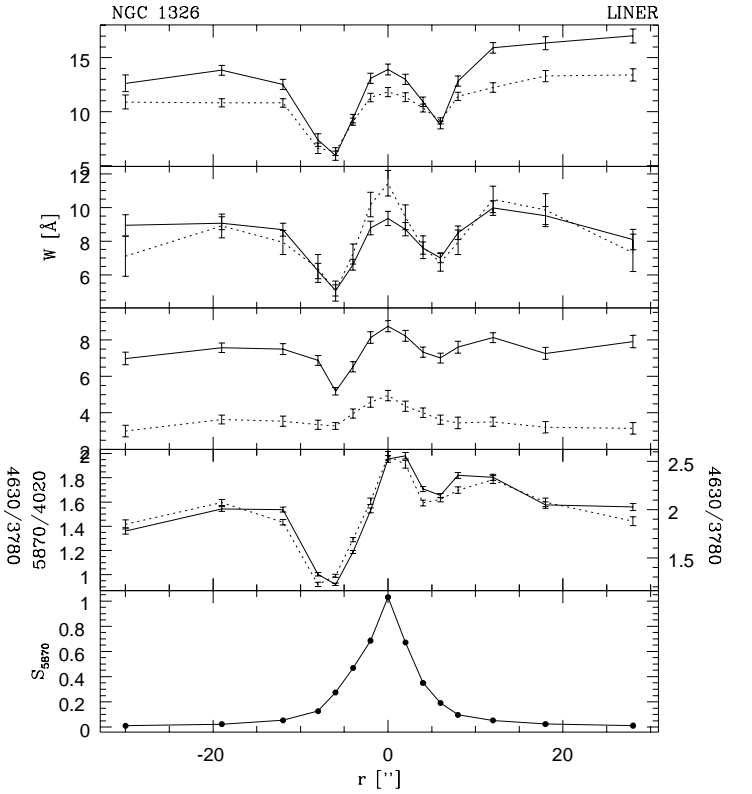


Figure 35. Same as Fig. 3.

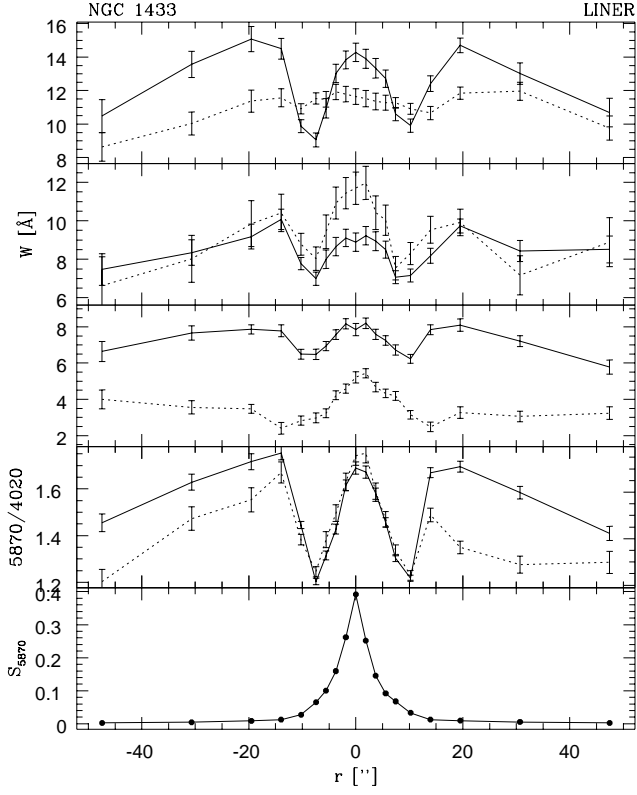


Figure 36. Same as Fig. 3.

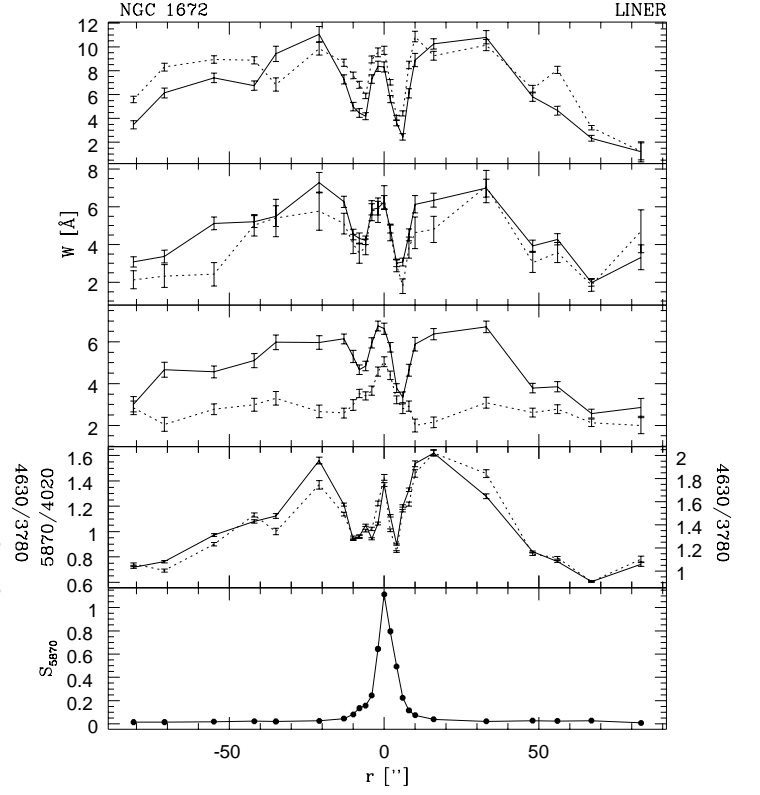


Figure 38. Same as Fig. 3.

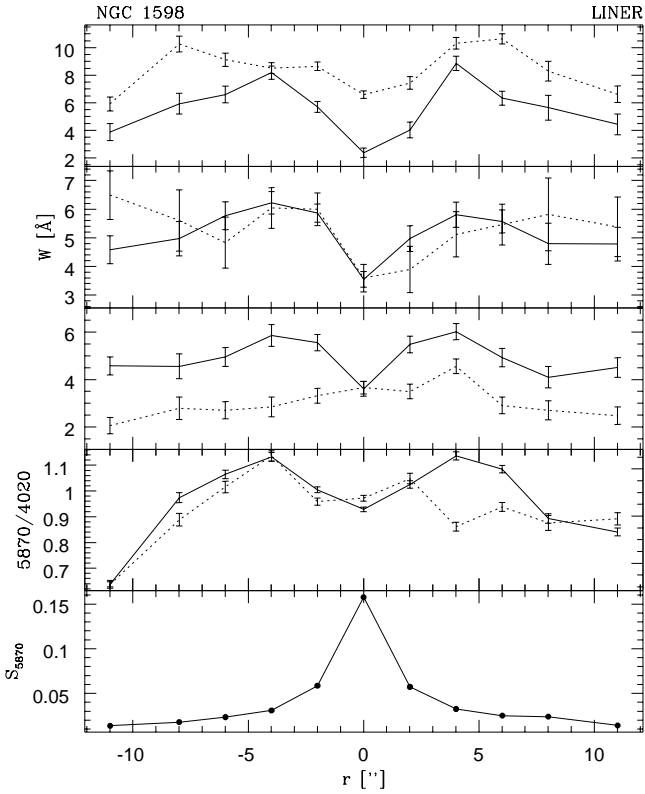


Figure 37. Same as Fig. 3.

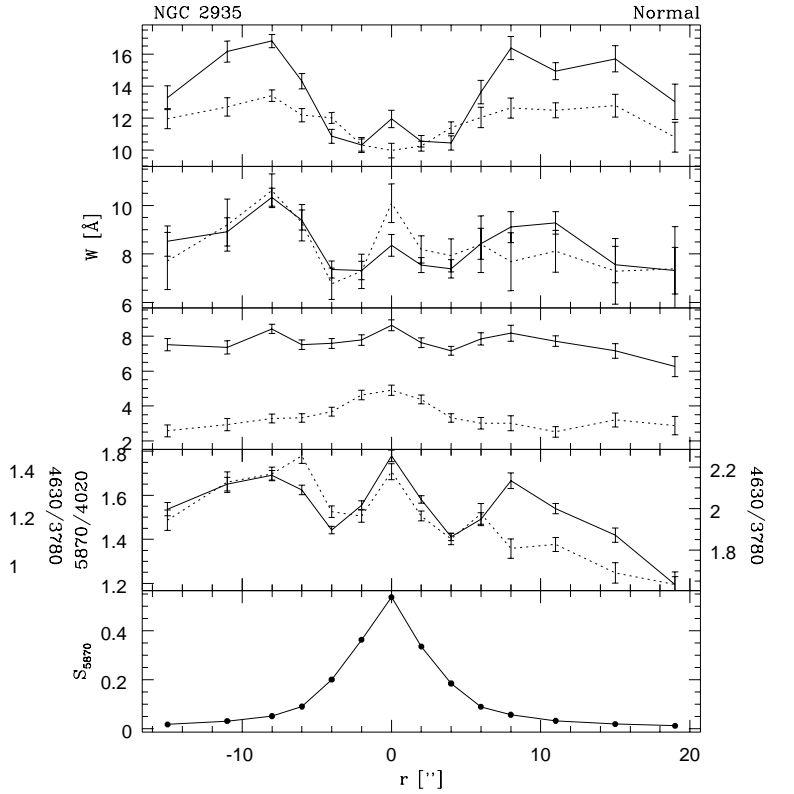


Figure 39. Same as Fig. 3.

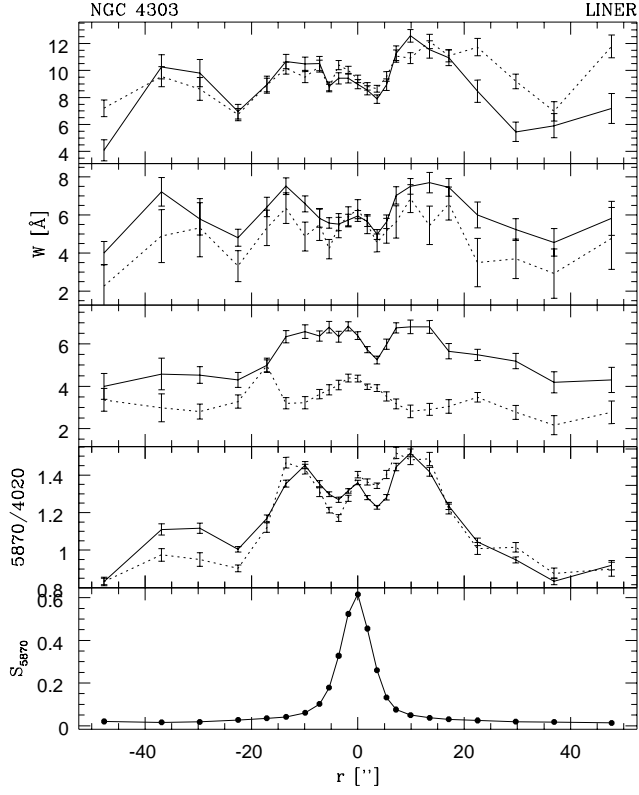


Figure 40. Same as Fig. 3.

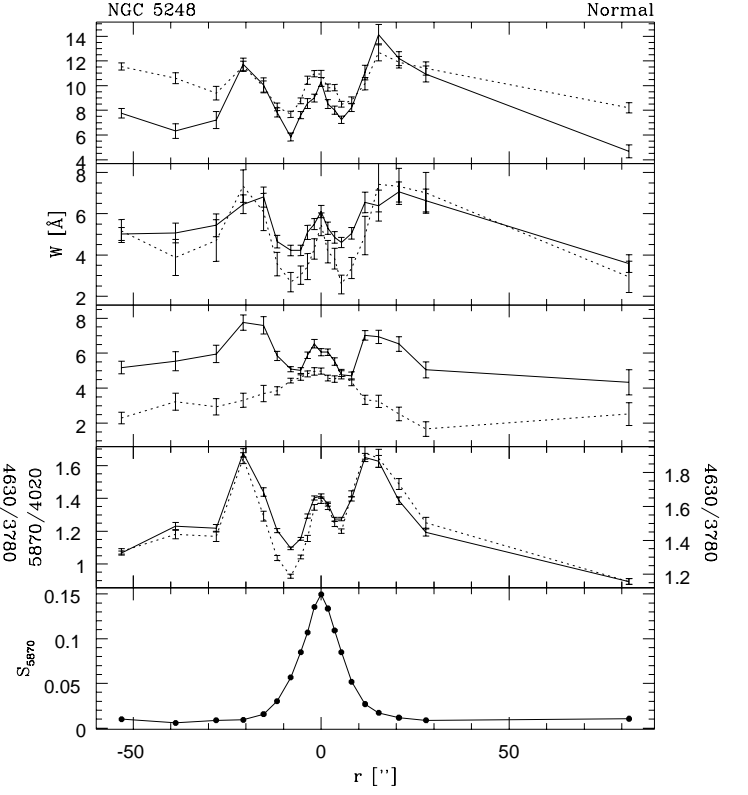


Figure 42. Same as Fig. 3.

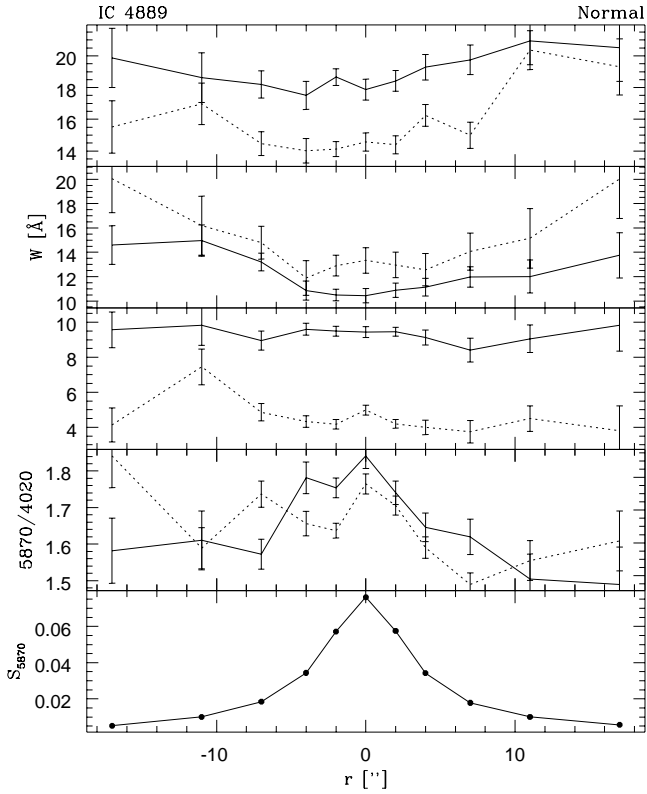


Figure 41. Same as Fig. 3.

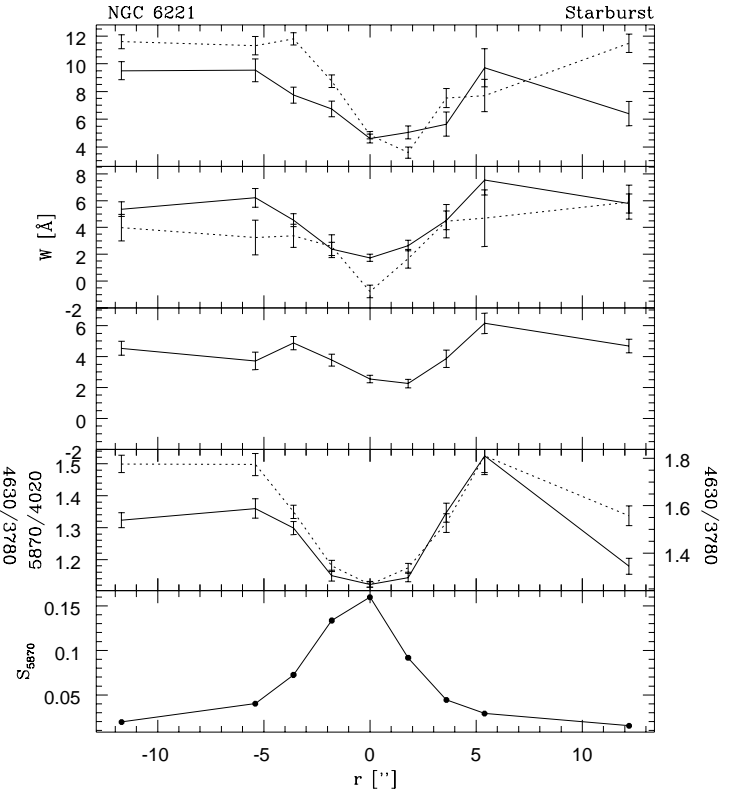


Figure 43. Same as Fig. 3.

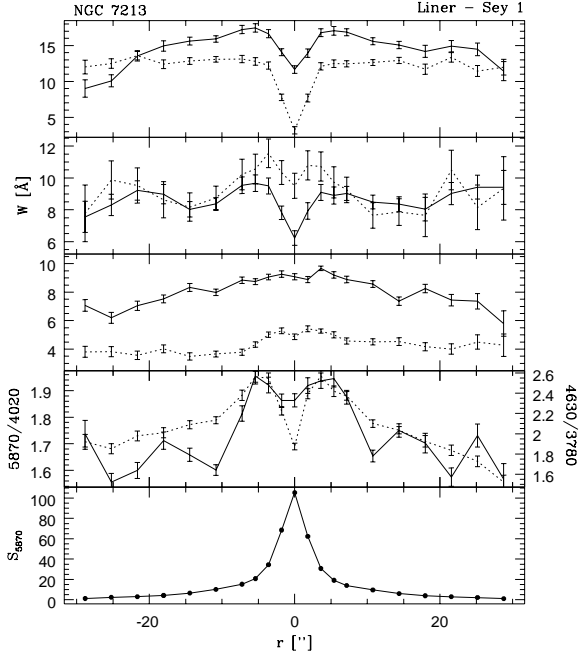


Figure 44. Same as Fig. 3.

One of the clearest examples of dilution by an AGN continuum in our data is NGC 6814 (Figs. 8 and 45c). The high degree of variability both in the lines and continuum of NGC 6814 (Yee 1980, Sekiguchi & Menzies 1990) are an unequivocal signature of the presence of an AGN in this galaxy. The presence of a FC is reflected in our  $W$  profiles, which show substantial dilution in the nucleus. Comparing the values of the nuclear  $W$ s with those between  $|r| = 5$  and  $11''$  we obtain dilution factors of 47% for Ca K, 28% for CN, 53% for the G-band and 22% for Mg. The larger dilution in the G-band is due to broad  $H\gamma$  entering the line window (Fig. 45c). The FC also affects the nuclear colors, which are bluer than in the neighboring regions (Fig. 8). The  $W$ s and continuum ratios at  $5''$  from the nucleus correspond to a S2–S3 template, changing to S5–S6 outwards. The attribution of a spectral template to the nucleus is not meaningful in this case given the obvious presence of a non-stellar continuum.

An interesting case of a galaxy showing signs of dilution is that of the LINER/Seyfert 1 NGC 7213 (Phillips 1979, Filippenko & Halpern 1984). Our  $W$  profiles show a clear drop in the  $W$ s of Ca K, CN and G-band, but not in Mg. (Ca H is also diluted, but mostly due to  $He$ .) This indicates that the FC is not strong enough in the  $5100 \text{ \AA}$  region to dilute the Mg line, but its contrast with the stellar component increases towards shorter wavelengths, resulting in a dilution of  $\sim 31\%$  of Ca K. This value is very similar to that obtained by Halpern & Filippenko (1984).

Apart from their dilution at the nucleus of the NGC 7213, the  $W$ s of Ca K and H, CN and G-band indicate a S2–S3 template at  $5''$  and outwards. Mg has a  $W$  similar to that of a S1 template at the nucleus, gradually changing to S4 in the outer regions. The continuum ratios are similar to a S2 template in the inner  $5''$  radius, decreasing to S3 in the outwards. The stellar population template obtained by Bonatto et al. (1989) is S2, similar to the values we obtained for the regions outside the nucleus.

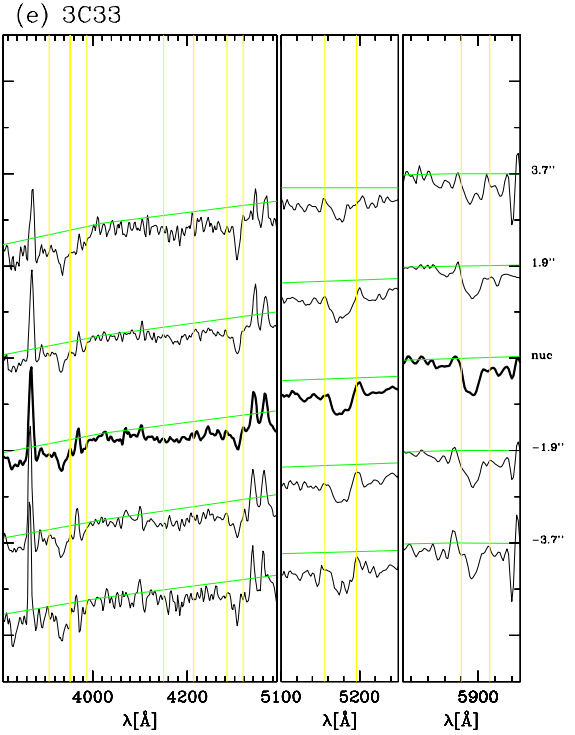


Figure 45. (cont.)

In Fig. 45b we show the spatially resolved, zoomed spectra of NGC 7213. The correspondence between the  $W$ s variations in Fig. 44 and the features in the individual spectra is clearly seen. The dilution of Ca K and H, CN and G band is observed as shallower absorption lines in the nuclear spectrum, while the lack of dilution in Mg can be noticed by the similar depths of the line in different extractions.

#### 4.1 Individual Objects

The five cases discussed above fully illustrate the potential of long slit spectroscopy as a tool to probe stellar population gradients and the presence of a featureless AGN-like continuum. In this section we provide a description of our results for the remaining objects in our sample, separated by activity class (Seyfert 1s, Seyfert 2s, Radio Galaxies, LINERs and Normal Galaxies).

##### 4.1.1 Seyfert 1s

**NGC 526a:** This is the brightest galaxy of a strongly interacting pair, which presents an optical emission line region elongated in the direction of the companion galaxy (NW–SE, Mulchaey et al. 1996). Both  $W$ s and continuum ratios of this galaxy present a mild gradient (Fig. 4), but opposite to that expected from dilution by a blue continuum. The  $W$ s are larger at the nucleus, indicating S3–S4 templates, decreasing outwards, with values of S4–S5 templates at  $7''$  from the nucleus. The continuum ratios indicate the same templates outside the nucleus but a redder ratio at the nucleus, corresponding to a S1 template.

**Figure 45.** Spectra of five of the sample galaxies for several positions along the slit, zoomed into the regions of the absorption features discussed in this work. (a) NGC 1672, (b) NGC 7213 (c) NGC 6814, (d) Mrk 573 and (e) 3C33. The radial positions are indicated on the right side of the plots.

**ESO 362-G18:** According to Mulchaey et al. (1996), this Seyfert 1 is a strongly perturbed galaxy, with the strongest [OIII] emission concentrated in the nucleus and showing an extension to the SE, suggestive of a conical morphology. The Ws and continuum ratios show a strong dilution by a FC in the nuclear region (Fig. 5). At 5'' and farther out, both Ws and continuum ratios indicate a S5 template.

**Mrk 732:** The individual spectra (Fig. 1) show signatures of young stars to the NE of the nucleus ( $r < 0$ ), where the Ws consistently indicate an S7 template. The nuclear Ws indicate a dilution when compared to the SW side ( $r > 0$ ), which shows Ws of a S5 template (Fig. 6). The continuum ratios indicate the same templates.

**MCG-02-33-034:** This galaxy was classified as Seyfert 1 by Osterbrock & De Robertis (1985), based on the appearance of permitted lines broader than the forbidden ones and strong FeII emission. Mulchaey et al. (1996) show that it presents evidence of two nuclei, both emitting in [OIII] and H $\alpha$ . We can see the dilution of Ws and color changes due to a blue FC in the nuclear region (Fig. 7). The Ws change to values of a S3 template at 4'' and outwards, while the continuum ratios have values similar to a S4 at 4'' and farther out. As noted in §3, though dilution clearly occurs, the complex nuclear spectrum (Fig. 2d) prevents an accu-

rate determination of both Ws and continuum at  $r = 0$  for this galaxy.

**NGC 6860:** According to L  pari, Tsvetanov & Macchetto (1993) the H $\alpha$  image of this galaxy shows bright emission line regions associated with the nucleus and a circum-nuclear ring of star-formation. The emission line spectrum is typical of a Seyfert 1.5 and variable. The Ws (Fig. 9) are diluted by a FC at the nucleus. Their values change to those of a S2 template at 4'' and outwards. The continuum ratios show a gradient in the opposite direction, decreasing from S4 in the inner 5'' radius to S5 outwards, bluer than the values indicated by the Ws in the outer regions.

#### 4.1.2 *Seyfert 2s*

**Mrk 348:** This is a Seyfert 2 galaxy with evidence of broad H $\alpha$  (De Robertis & Osterbrock 1986b), HeI 10830    and Pa   lines (Ruiz, Rieke & Schmidt 1994). Koski (1978) observed this galaxy through a 2.7'' $\times$ 4'' aperture, obtaining a 14% contribution from a FC at 5000   . Kay (1994) estimated a FC contribution of 35% to the flux at 4400   , while Tran (1995a) finds 27% at 5500   . Mrk 348 is one of the Seyfert 2 galaxies which had a hidden Seyfert 1 nucleus revealed by spectropolarimetry (Miller & Goodrich 1990).

The Ws and continuum ratios of this galaxy are shown

Figure 45. (cont.)

in Fig. 10. The Ws have values similar to those of a S4 template, without any noticeable gradient in the inner  $8''$ . From Koski (1978), Kay (1994) and Tran (1995a) results, we would expect the Ws to be substantially diluted in the nuclear region, but this is not detected. One possibility would be that the FC is extended, diluting *all* the Ws. However, the NLR of this galaxy is extended by less than  $2''$  (Schmitt & Kinney 1996), and the FC would have to be extended by  $\approx 8''$ .

The continuum ratios show a gradient, having values similar to those of a S4 template at the nucleus and becoming bluer outwards, reaching values similar to those of S5–S6 templates. The continuum behavior of Mrk 348 is intriguing, due to the fact that outside the nucleus it indicates bluer templates than the ones expected from the analysis of the Ws. This behavior is also seen in many other objects in the present sample, particularly Seyfert 2s.

**Mrk 573:** Pogge & De Robertis (1993) found excess near-UV emission, spatially extended along the [OIII] emission, interpreted as scattered nuclear continuum. Koski (1978) estimated that the FC contributes 12% of the light at  $5000 \text{ \AA}$ , observed through a  $2.7'' \times 4.0''$  aperture, while Kay (1994) finds 20% FC at  $4400 \text{ \AA}$  within an aperture of  $\approx 2 \times 6''$ . She also estimated, based on spectropolarimetry, that the FC is polarized by 5.6% in the  $3200\text{--}6300 \text{ \AA}$  range, in agreement with the values found by Martin et al. (1983).

The Ws (Fig. 11) show a mild gradient, from a S3 template at the nucleus, to a bluer one, S4 at  $5''$ . The continuum ratios show a gradient from a S3–S4 template at the nucleus

to a bluer one, S5–S6 at  $5''$ . Koski (1978) and Kay (1994) estimations of FC continuum contribution to the nuclear spectrum are not confirmed by our data, which do not show any detectable dilution in the Ws. This galaxy is another case in which the continuum ratios outside the nucleus have values bluer than we would expect from the Ws analysis.

**IC 1816:** This galaxy was identified as a Seyfert 1 by Fairall (1988), but the lack of variability led Winkler (1992) to question this classification. Our spectrum does not show broad emission lines, which lead us to classify it as a Seyfert 2. The Ws of this galaxy (Fig. 12) have values typical of S3 templates in the inner  $4''$ , with an *apparent* dilution in Mg caused by contamination by [NI] emission. The Ws decrease to values of a S5 template at  $8''$  from the nucleus. The continuum ratios have values corresponding to templates bluer than the Ws, S5 at the nucleus, changing to S6 at  $8''$ .

**ESO 417-G6:** Our spectrum was obtained with the slit oriented along the extended emission (NW–SE direction, according to Mulchaey et al. 1996). The Ws show no gradient (Fig. 13), having values typical of a S3 template. The *apparent* dilution in the Mg band is due to contamination by [NI] emission. The continuum ratios show a gradient, changing from S3 at the nucleus, to a bluer S5 template at  $\approx 5''$  from the nucleus.

**Mrk 607:** According to De Robertis & Osterbrock (1986a) the nuclear spectrum of this galaxy shows high-excitation lines, like [FeVII] and [FeX], but only narrow permitted lines. Kay (1994) obtained a 10% FC contribution to

the nuclear flux, and estimates a 4.3% continuum polarization in the 3200–6300 Å range.

The Ws and continuum ratios (Fig. 14) indicate similar templates, S2–S3 at the nucleus, S5 at 6'', suggesting a weak starforming ring, and S3 outwards. Our spectrum of this edge-on galaxy was obtained with the slit positioned along the major axis, which may explain the large variations in the Ws in such small scales. Considering these variations, we cannot evaluate whether the nuclear Ws are diluted or not.

**NGC 1358:** The nuclear FC contributes with 17% of the flux and is polarized by 1.7% in the 3200–6300 Å range, according to Kay (1994). The Ws of NGC 1358 (Fig. 15) show no systematic gradient and have values typical of a S1 template, the same result obtained by Storchi-Bergmann & Pastoriza (1989). The only exception is Ca K, which reaches values larger than S1 at  $r = -6''$ . The continuum ratios show a gradient from values typical of a S1 template at the nucleus to bluer values typical of a S5 template outwards. This galaxy is another case in which the continuum ratios outside the nucleus have values bluer than the ones expected from the analysis of the Ws.

**NGC 1386:** The Ws are typical of a S3 template at the nucleus (Fig. 16), S4–S5 at 10'' from the nucleus, due to the presence of spiral arms (Storchi-Bergmann et al. 1996a), and S3 outwards. The continuum ratios indicate a S1 template at the nucleus, with a gradient to values typical of S5–S6 at 10'' and outwards.

**CGCG 420-015:** This galaxy was classified as Seyfert 2 by de Grijp et al. (1992). The W values are indicative of a S3 template at the nucleus, with G-band and Mg showing a small gradient to S2 outwards, consistent with a small dilution in the nucleus (Fig. 17). The continuum ratios indicate a S1 template at the nucleus, redder than the value predicted from the Ws, with a gradient to S3–S4 at 4'' and farther out. Care must be taken when analyzing the Ws and continuum ratios of this galaxy, because it was observed with the slit positioned almost perpendicular to the parallactic angle, introducing large differential refraction effects.

**ESO 362-G8:** The Ws are similar to a S5–S6 template at the nucleus, with a gradient to S4–S5 at 4'' and farther out (Fig. 18). The continuum ratios are similar to a S5 template at the nucleus, changing to bluer values, typical of S6–S7 templates outwards. The Ws of this galaxy indicate bluer templates in the nuclear region, which is due to the presence of young stars, revealed by strong H I absorption features. This galaxy also has continuum ratios outside the nucleus bluer than the values predicted from the Ws.

**Mrk 1210:** Tran, Miller & Kay (1992) found polarized broad H $\alpha$  and H $\beta$  components in the spectrum of this galaxy. Later Tran (1995a,b,c) confirmed this result and determined that the FC contributes to 25% of the nuclear flux at 5500 Å, while Kay (1994) estimates a 64% FC contribution at 4400 Å. Nevertheless, the Ws show almost no gradient indicative of such a dilution (Fig. 19). The Ws correspond to S4 and S5 templates. The continuum ratios are similar to S5–S6 at the nucleus, with a gradient to S6 outwards, which is bluer than the template estimated from the Ws. There is an *apparent* dilution of the Mg and Na features in the nuclear spectrum due to emission line contamination by [NI] and He I respectively.

**NGC 3081:** This galaxy was classified as a Seyfert 2

by Phillips, Charles & Baldwin (1983). According to Pogge (1989a), the [OIII] image is symmetrical but more extended than the stars profile. The W profiles (Fig. 20) do not show any evidence of a stellar population gradient, with values similar to S2–S3 templates. The continuum ratios show a gradient from a S2–S3 template at the nucleus, to S4–S5 at 5'' and outwards, bluer than the values indicated by the Ws.

**IRAS 11215-2806:** This galaxy was classified by de Grijp et al. (1992) as a Seyfert 2. The Ca K and G-band Ws (Fig. 21) present a gradient from a S4 template at the nucleus to S2 in the outer regions, indicating dilution by a blue continuum. Mg presents almost no gradient, with values typical of S3–S4 templates. The continuum ratios present a gradient in the opposite direction, from S4 at the nucleus, to S5 outwards.

**MCG-05-27-013:** This galaxy was classified as Seyfert 2 by Terlevich et al. (1991). The Ws of Ca K are typical of a S3 template at the nucleus, changing to S1 outwards, which suggests dilution by a FC (Fig. 22). The G-band has a smaller gradient, with values similar to a S2 template at the nucleus and S1 outwards, while for Mg the values are similar to a S2 template, with no gradient. The continuum ratios have values larger than S1 at the nucleus, due to strong reddening, changing to values similar to S4 in the outer regions, bluer than the values predicted by the analysis of the Ws.

**Fairall 316:** This is a Seyfert 2 galaxy discovered by Fairall (1981). The Ws show no gradient (Fig. 23), with Ca K having values typical of S2, while G-band and Mg have values typical of S1. The continuum ratios have values of S1 template at the nucleus, decreasing outwards to values bluer than those predicted by the Ws, similar to a S3 template.

**NGC 5135:** NGC5135 was described by Phillips, Charles & Baldwin (1983) as having a *composite* nucleus with characteristics of both Seyfert 2 and Starburst. Thuan (1984) obtained IUE spectra of this galaxy, confirming the dual nature of the nucleus, which presents both emission lines typical of Seyfert 2s and absorption lines typical of Starbursts, the latter component contributing with 25% of the total UV emission.

The Ws (Fig. 24) show a gradient from values typical of a S7 template at the nucleus to S6–S5 at 7''. The continuum ratios also show a gradient from S6 at the nucleus to S5 at 7''. This gradient is due to the presence of young stars in the nuclear region, as revealed by strong H I absorption features.

**NGC 5643:** This galaxy was classified by Phillips et al. (1983) as a low luminosity Seyfert 2. Schmitt, Storchi-Bergmann & Baldwin (1994) presented [OIII] and H $\alpha$  images, as well as optical spectra of NGC5643. The images show the high-excitation gas to be extended along the E-W direction by  $\approx 20''$ . The stellar population is moderately old in the central region, showing evidence of absorption lines diluted by a blue continuum, supposed to be scattered nuclear light.

The Ws of this galaxy present a mild gradient to the E of the nucleus (i.e., towards negative  $r$  in Fig. 25), suggesting the presence of scattered light up to at least 4'' from the nucleus. In the outer regions, the Ws correspond to templates S3–S4, while the continuum ratios correspond to S3 to the E of the nucleus and S1 to the W. Bonatto et al. (1989) obtained that the nuclear stellar population of this galaxy can be represented by a S3 template, similar our result.

**NGC 6300:** Storchi-Bergmann & Pastoriza (1989) ob-

served the nuclear stellar population of this galaxy to be old, with a small contribution from intermediate age stars. The Ws do not show a clear gradient (Fig. 26), with Ca K varying between S2 and S3 templates, while G-band and Mg vary between S4 and S5. The continuum ratios decrease from values much larger than those of a S1 template at the nucleus to values typical of a S6 template at  $10''$  and farther out, bluer than the values predicted from the Ws in this region.

**NGC 6890:** Storchi-Bergmann, Bica & Pastoriza (1990) studied the nuclear optical spectrum of this galaxy, finding that the stellar population is old and that H $\alpha$  may have a broad component. The Ws show a gradient in Ca K and G band, which change from S4 at the nucleus to S3 in the outer regions, but not in Mg, which has values typical of a S3 template, with no gradient (Fig. 27). The continuum ratios have values larger than S1 at the nucleus, decreasing to S2 in the outer regions. These results are similar to the ones obtained by Storchi-Bergmann, Bica & Pastoriza (1990).

**NGC 7130:** Like NGC 5135, this galaxy has a Seyfert 2 nucleus surrounded by a Starburst (Phillips et al. 1983). Thuan (1984) presents IUE spectra which show both high-excitation emission lines typical of Seyfert 2s and absorption lines typical of Starburst. The starburst component dominates the UV emission, with  $\approx 75\%$  of the flux. Shields & Filippenko (1990) showed that the narrow line region have two kinematical components and emission line ratios which vary from those of AGN in the nucleus to those typical of HII regions outwards.

Both Ws and continuum ratios show a marked gradient (Fig. 28). The Ws change from values similar to S7 at the nucleus to S6 outwards, while the continuum ratios change from S6–S7 at the nucleus to S5–S6 outwards. This gradient is due to the presence of a circumnuclear star-forming region.

**NGC 7582:** Morris et al. (1985) found circumnuclear H $\alpha$  emission in this Seyfert 2 galaxy, suggesting a ring of rotating HII regions in the galaxy plane. The Ws of this galaxy show a dilution, changing from S7 at the nucleus to S3–S4 in the outer regions (Fig. 29). The continuum ratios are similar to S3 at the nucleus and NE ( $r < 0$ ), but decrease to values similar to S5–S6 towards  $r > 0$ . The continuum ratios to the SW are bluer than what we would expect from the Ws results. The dilution measured in this object is probably due to its inner star-forming ring.

#### 4.1.3 Radio Galaxies

**3C 33:** This is a FR II radio source. Koski (1978) estimated that the FC contributes to 19% of the flux at 5000 Å, observed through a  $2.7'' \times 4''$  aperture. Antonucci (1984) obtained spectropolarimetric data, which shows wavelength independent polarization, but no broad polarized emission lines.

The Ws of this radio-galaxy (Fig. 30) have values similar to an E3 or E6 template, though W(MgI) is more similar to an E1 template. The continuum is redder at the nucleus, with values of an E2 template, decreasing to values typical of an E3 or E6 template outwards. The FC contribution estimated by Koski (1978) would produce a dilution of the Ws in the nuclear region. Our data do not support this result, as the W-profiles are essentially flat.

**Pks 0349-27:** The Ws (Fig. 31) do not show a gradient and have values typical of an E1–E2 template, whereas the continuum ratios show a gradient from an E2 template at the nucleus to a bluer, E3–E4 template outwards.

**Pictor A:** This is a FR II Broad Line Radio Galaxy with a strong double lobed radio source oriented along the E–W direction (Christiansen et al. 1977). Halpern & Eracleous (1994) detected double-peaked Balmer lines, not present in previous spectra. The Ws and continuum ratios (Fig. 32) show a strong dilution by the FC at the nucleus. Their values correspond to a S4 template outwards, except for the G-band, where the values are similar to those of a S1 template in the outer regions. The remarks about the uncertain continuum and W measurements in the nucleus of MCG-02-33-034 also apply to Pictor A.

**Pks 0634-20:** This is a FR II radio source. Simpson, Ward & Wilson (1995) did not detect a broad Pa $\alpha$  line and show that the K–L color, [OIII] and soft X-ray fluxes are consistent with the spectral energy distribution of a quasar absorbed by  $A_V \approx 30$  mag. The Ws (Fig. 33) are consistent with an E2 stellar population, without a gradient. The continuum ratios indicate bluer templates, E3 at the nucleus, decreasing to values typical of E6 outwards.

**Pks 0745-19:** According to Baum & Heckman (1989), this narrow line radio galaxy does not have a well defined FR class. The Ws indicate an E8 template at the nucleus, with a gradient to values typical of E4 outwards (Fig. 34), suggesting dilution by a FC. The continuum ratios indicate a redder, E2 stellar population. However, it should be noticed that these continuum ratios were not corrected by foreground reddening, because this galaxy lies too close to the Galactic plane ( $b < 4^\circ$ ).

#### 4.1.4 LINERs and Normal Galaxies

**NGC 1326:** Storchi-Bergmann et al. (1996a) obtained narrow band [OIII] and H $\alpha$  images, which reveal a circumnuclear ring at  $|r| \approx 6''$ . As for NGC 1097 and other galaxies containing star-forming rings, the Ws and color profiles of this galaxy (Fig. 35) confirm the presence of a ring. The radial behavior of the Ws and continuum ratios do not evidence the presence of a FC in the nucleus. The Ws have values typical of a S3 template at the nucleus, S6 at the ring and S2–S3 outwards. The continuum ratios indicate a S1 template at the nucleus (redder than the one indicated by the Ws), S6 at the ring, and S3–S4 outwards.

**NGC 1598:** According to Phillips et al. (1984), the nuclear spectrum of this galaxy is similar to that of LINERs, with evidence of young stars at the nucleus, which is also surrounded by a ring of HII regions. The Ws and continuum ratios (Fig. 37) indicate similar templates: S7 at the nucleus, in agreement with the presence of young stars, and S5 from 4 to  $6''$  reaching values typical of a S6 template outwards.

**NGC 2935:** This is a normal galaxy with a nuclear ring of star formation (Buta & Crocker 1992). The Ws of Ca K and G-band are similar to S4 at the nucleus, S5 at the ring ( $5''$ ) and S2 outwards, while Mg is similar to S2 at the nucleus, S3 at the ring and S2 outwards (Fig. 39). The continuum ratios are similar to S3 at the nucleus, S5 at the ring and S3 outwards.

**NGC 4303:** This is a Sersic-Pastoriza galaxy, classified

as a LINER by Huchra, Wyatt & Davis (1982). Filippenko & Sargent (1985) observations show that HII regions are prominent in the nucleus and circumnuclear region. They also found a substantially broader component in each line and propose we are seeing a faint Seyfert 2 or LINER nucleus hidden by HII regions.

The Ws are similar to a S5 template at the nucleus, decreasing to values similar to a S6 template at the ring (5''; Fig. 40). From 7'' to 15'' from the nucleus the Ws are similar to a S4 template, decreasing to S6–S7 in the outer regions. The continuum ratios behave like the Ws, with the exception of the nucleus and ring, where they indicate redder templates, S4 and S5 respectively. In the other regions Ws and continuum ratios indicate similar templates. Our results are in good agreement with those of Bonatto et al. (1989).

**IC 4889:** Phillips et al. (1986) found H $\alpha$ , [NII] and [OII] emission in this normal elliptical galaxy. The Ws show no significant gradient, with values typical of an E1 template, while the continuum ratios are E1 at the nucleus and decrease to values similar to those of an E3 template in the outer regions (Fig. 41).

**NGC 5248:** Both Ws and continuum ratios show the presence of a ring at  $|r| = 10''$  from the nucleus (Fig. 42). The values of Ca K and G-band are typical of a S5 template at the nucleus, S6 at the ring, S4 at 15'' from the nucleus, decreasing to values typical of S6–S7 templates outwards. Mg and continuum ratio values indicate redder templates, S4 at the nucleus, S5 at the ring, S2–S3 at 15'', decreasing to S5–S6 outwards. Our result for the nuclear stellar population is similar to the one obtained by Bonatto et al. (1989).

**NGC 6221:** This southern spiral galaxy was classified as a Seyfert 2 by Véron, Véron & Zuiderwijk (1981) and Pence & Blackman (1984), based on the detection of a faint broad H $\beta$  component, an [OIII] line broader than H $\beta$  and to the proximity to a hard X-ray source (Marshall et al. 1979, Wood et al. 1984). However, Schmitt & Storchi-Bergmann (1995) recently proposed that the identification of NGC6621 with the X-ray source is probably wrong and that it would rather be related to the high-excitation Seyfert 2 galaxy ESO138-G01. Pence & Blackman (1984) data also show that the nucleus is surrounded by a Starburst.

Our W profiles (Fig. 43) show a gradient from a S7 template at the nucleus to S5 at 5'' and farther out, in agreement with the presence of a nuclear starburst, confirmed by the gradient also observed in the continuum ratios, which correspond to S6 at the nucleus and to S5 at 5'' and farther out.

## 5 DISCUSSION

The present set of high quality long-slit spectra contains a wealth of information on the properties of AGN and of the stellar population of their host galaxies. In this section we discuss some of the global results revealed by our analysis and their possible implications.

### 5.1 Stellar Populations

The values of the continuum colors and Ws of the stellar lines found in our analysis cover a wide range, as can be seen in Figs. 3–44. Even in inner regions of the bulge not affected

by circumnuclear star-formation or by a non-stellar FC, the galaxies exhibit substantial differences in the Ws and colors, reflecting a variety of stellar population properties. This was confirmed by our characterization of the spectra in terms of Bica's (1988) templates, which showed that, despite a predominance of S2 and S3 templates, every spectral type from S1 to S7 appears in the representation of the spectra in the inner regions of our sample galaxies.

This observed *variety* of stellar population properties illustrates the inadequacy of using a single starlight template to evaluate and remove the stellar component from AGN spectra. The importance of an accurate evaluation of the starlight component cannot be underestimated. A 'template mismatch' affects not only the derived emission line fluxes, but also, and more strongly, the determination of the strength and shape of a residual FC. We have seen, for instance, that many of the nuclei in the present sample show no evidence for dilution of the stellar lines in comparison with off-nuclear spectra of the same galaxy. However, some dilution would most probably be measured if a different galaxy was used as a starlight template. The cases of Mrk 348, 573, 1210 and 3C33 are illustrative in this respect. Whereas Koski (1978), Kay (1994) and Tran (1995a) obtained large contributions of a FC comparing their spectra with a normal galaxy template (§4.1), we find little evidence for dilution of the absorption lines comparing the nuclear Ws with those measured a few arcseconds outside the nucleus.

This brings up the question of which is the best way to estimate the stellar component in an AGN spectrum. By far the most commonly adopted procedure is to use the spectrum of a normal galaxy as a starlight template. Given the variety of stellar populations found in AGN, if a template galaxy is to be used at all then it has to be chosen among a library contemplating a large variety of stellar population characteristics. An alternative technique, implicitly used in this paper, is to use an off-nucleus spectrum of the object as the starlight template. This is arguably a more robust method, as the best representation of the stellar population in a given galaxy is the galaxy itself! The extrapolation to zero radius, however, involves the assumption that the stellar population in the bulge of the host galaxy does not change dramatically in the inner few arcseconds. A comparison between these two methods of starlight evaluation will be presented in a future communication.

### 5.2 Dilution factors

Figs. 3–44 demonstrate that several galaxies show signs of dilution of the stellar lines in the nucleus. In this section we compare the nuclear Ws to those a few arcseconds outside the nucleus in order to estimate the fraction of the continuum associated with a featureless spectral component.

In order to obtain Ws representative of the neighbourhood of the nucleus we have co-added typically four extractions, two in each side of the nucleus, located at distances ranging from 2 to 12'' (see Table 4). Extractions adjacent to the nucleus were avoided whenever possible, since, due to seeing, they are often contaminated by the nuclear spectrum. The typical distance of the off-nuclear extractions was 4'', corresponding to physical radii between  $\sim 0.5$  and 2 kpc for the distances of the galaxies in the sample.

After constructing these off-nuclear templates and mea-

asuring their  $W_s$ , the FC fraction of the total continuum spectrum at the wavelength of an absorption line was estimated by

$$f_{\text{FC}}(\lambda) = \frac{W_{\text{off-nuc}} - W_{\text{nuc}}}{W_{\text{off-nuc}}} \quad (1)$$

where  $W_{\text{nuc}}$  and  $W_{\text{off-nuc}}$  are the  $W_s$  in the nucleus and in the off-nuclear template respectively.

Table 4 presents the results of this analysis. Galaxies not listed in Table 4 show no signs of dilution, and even for some objects in the table (e.g., NGC 1097, Mrk 348) the evidence for dilution is only marginal—by ‘marginal’ we mean within  $2\sigma$  of a spurious dilution caused by the errors in the  $W$  measurements. We recall that dilution of the  $W_s$  by less than 10% cannot be reliably detected with this method due to the errors in the  $W_s$ . We concentrated this analysis in the Ca K, G-band and Mg lines. However, as indicated in the Table, the Mg line is very often contaminated by [Fe VII] and/or [NI] in the nuclear spectrum, producing an *apparent* dilution. In such cases the  $f_{\text{FC}}(5176\text{\AA})$  fractions have to be taken as upper limits of the actual dilution. The line which is less affected by such spurious effects is Ca K. Empty slots in Table 4 occur whenever an increase in the  $W$ , instead of dilution, was observed.

Of the broad-lined objects in our sample, only NGC 526a does not exhibit a systematic dilution of the  $W_s$  in the nucleus. The other possible exception is NGC 1097, which does show some dilution in the Ca K line, but at a marginal level. The highest values of  $f_{\text{FC}}$  occur for MCG-02-33-034 and Pictor A, where it reaches nearly 80% at the wavelength of Ca K. However, as discussed in §3, these values are not as reliable as for other Seyfert 1s due to the uncertain positioning of the continuum for these two objects. Indeed, their nuclear spectra are so complex that the G-band and Mg lines are completely filled by emission, preventing a determination of  $f_{\text{FC}}$  at the corresponding wavelengths.

Perhaps the most intriguing aspect of Table 4 is the low degree of dilution detected in Seyfert 2s. Of the 20 Seyfert 2s in our sample, 13 are listed in Table 4, and only 9 of these (IC 1816, ESO 362-G8, NGC 5135, 5643, 6890, 7130, 7582, MCG -05-27-013 and IRAS 11215-2806) have dilution convincingly detected. As reviewed in §4.1, NGC 5135, 7130, 7582 and ESO 362-G8 are composite nuclei, showing features of both Seyfert 2s and Starbursts. In these cases, as for the LINER NGC 1598 (Fig. 37), the dilution is almost certainly dominated by the young stellar component, not a genuine AGN continuum. This lowers the count to 5 objects with detected dilution out of 16 ‘pure’ Seyfert 2s. Marginal indications of dilution were found in Mrk 348, Mrk 1210, NGC 1358 and CGCG 420-015. In the other objects, the FC, if present at all, contributes 10% or less in the optical. This result is further discussed below.

### 5.2.1 Implications for FC2

The low levels or lack of dilution in Seyfert 2s found in the present analysis is an interesting result in light of the current debate over the existence and origin of a FC in Seyfert 2s and its implications for unified models. It has been shown that the FC in Seyfert 2s cannot be simply the continuum of a hidden AGN scattered into our line of sight, otherwise broad emission lines should also be seen, in contradiction

with the very definition of type 2 Seyferts (Cid Fernandes & Terlevich 1992, 1995, Heckman et al. 1995). Furthermore, the low levels of polarization (Miller & Goodrich 1990), and the observation of reflected broad lines substantially more polarized than the FC (Tran 1995c) are also in conflict with the simple obscuration/reflection picture.

These facts lead to the idea that a *second* FC component (dubbed FC2 by Miller 1994) must be present in Seyfert 2s. The nature of this component remains unknown, though both a circumnuclear starburst (Cid Fernandes & Terlevich 1995, Heckman et al. 1995) and free-free emission from the scattering region (Tran 1995c) have been suggested.

Our observations seem to indicate that a FC (and consequently FC2) is *not* an universal phenomenon in Seyfert 2s, and that previous determinations of the FC strength have been overestimated. A smaller FC contribution would alleviate, if not completely solve, all problems listed above.

A good way to further investigate this issue would be to obtain spectropolarimetry for the Seyfert 2s in the present sample. We expect galaxies for which no dilution of the  $W_s$  was detected to show little or no polarization. IC 1816, NGC 5643, NGC 6890, MCG -05-27-013 and IRAS 11215-2806, on the other hand, should exhibit large polarizations and Seyfert 1 features in the polarized spectra. In the cases of composite nuclei, spectropolarimetry could help disentangling the starburst and Seyfert 2 components and possibly reveal a hidden AGN.

As a final word of caution, we note that while throughout this paper we have attributed the dilution of absorption lines in the nucleus of active galaxies to a FC, dilution can also be caused by young stars, as shown to occur in circumnuclear star forming rings (e.g., Figs. 3, 36 and 38) and in the nuclei of the Starburst galaxies NGC 6221 and 7130 (Figs. 43 and 28). It is a known problem in optical spectroscopy of AGN that it is often difficult to distinguish between a young stellar population and a FC (e.g., Miller & Goodrich 1990, Cid Fernandes & Terlevich 1992, Kay 1994). UV spectroscopy offers the most direct way of removing this ambiguity (e.g., Leitherer, Robert & Heckman 1995, Heckman et al. 1995).

### 5.2.2 Metallicity gradients

In measuring the dilution of absorption lines with respect to their strengths  $\sim 4''$  (or  $\sim 1$  kpc) outside the nucleus we are making the assumption that the stellar population in the bulge of the host galaxy does not change appreciably from  $r \sim 4''$  to  $r = 0$ . This approximation might not be valid if the galaxy presents a strong metallicity ( $Z$ ) gradient, leading to an increase of the  $W_s$  towards the nucleus (e.g., Díaz 1992). If such a gradient is present, then a flat  $W$  profile as the one found in many of our galaxies could reflect the compensating effects of a FC diluting the enhanced metal lines in the nucleus<sup>§</sup>. In this section we investigate this possibility by means of an approximate treatment of the potential effects of a metallicity gradient.

To estimate the  $Z$ -gradient we have used  $\Delta \log Z / \Delta \log r = 0.2$ , a typical value obtained for  $r \gtrsim 3''$  in elliptical galaxies (Davies, Sadler & Peletier 1993

<sup>§</sup> We thank Dr. R. Terlevich for pointing this out to us.

DILUTION FACTORS					
Object	Type	$r$ ["]	$f_{\text{FC}}(\lambda)$ [%]		
			3930 Å	4301 Å	5176 Å
NGC 1097	Lin-1	4.0	6±5	-	-
NGC 1598 <sup>c</sup>	Lin	4.0	73±4	39±6	39±6
NGC 7213	Lin-1	3.6–7.2	31±4	33±6 <sup>b</sup>	-
ESO 362-G18	1	7.0–12.0	46±6	59±5 <sup>b</sup>	22±6 <sup>a</sup>
NGC 6814	1	5.0–10.8	47±4	53±6 <sup>b</sup>	22±5 <sup>a</sup>
MCG-02-33-034	1	4.0–7.0	76±5	100 <sup>b</sup>	100 <sup>a</sup>
NGC 6860	1	4.0–7.0	51±4	64±6 <sup>b</sup>	50±5
Pictor A	BLRG	3.7–6.5	77±3	100 <sup>b</sup>	100 <sup>a</sup>
Mrk 348	2	1.9–3.7	1±5	9±6	9±7 <sup>a</sup>
Mrk 1210	2	4.0–8.0	11±6	12±7	26±7 <sup>a</sup>
IC 1816	2	4.0	13±5	15±6	30±5 <sup>a</sup>
ESO 362-G8 <sup>c</sup>	2	4.0–7.0	25±6	15±7	11±5
NGC 1358	2	4.0–6.0	0±5	1±7	-
NGC 5643	2	3.6–5.4	19±4	33±6	33±4 <sup>a</sup>
NGC 6890	2	1.8–3.6	17±5	39±7	-
CGCG 420-015	2	2.0–4.0	4±5	15±6	5±7 <sup>a</sup>
IRAS 11215-2806	2	4.0–7.0	24±4	34±5	30±5 <sup>a</sup>
MCG-05-27-013	2	4.0–7.0	10±5	12±7	-
NGC 5135 <sup>c</sup>	2-SB	3.6–7.2	37±8	51±7	36±8 <sup>a</sup>
NGC 7130 <sup>c</sup>	2-SB	3.6–7.2	47±5	62±6	35±5 <sup>a</sup>
NGC 7582 <sup>c</sup>	2-SB	4.0–8.0	70±4	60±6	57±5 <sup>a</sup>
NGC 6221 <sup>c</sup>	SB	3.6–5.4	52±4	73±4	49±6 <sup>a</sup>
PKS 0745-19	NLRG	1.9	55±13	3±20	15±11 <sup>a</sup>

**Table 4.** Column 3 lists the range in distances from the nucleus used to compute  $W_{\text{off-nuc}}$ . Columns 4–6 list the FC fractions corresponding to the Ca K, G-band and Mg lines respectively.

<sup>a</sup> contamination by [FeVII] and/or [NI].

<sup>b</sup> contamination by broad H $\gamma$ .

<sup>c</sup> dilution due to young stars in the nucleus.

and references therein). Assuming that the nuclear stellar population sampled in our  $2'' \times 2''$  aperture is characterized by a mean radius of  $0.5''$ , and considering a typical off-nuclear extraction distance of  $4''$ , this corresponds to an increase of  $\sim 0.2$  dex in  $Z$  from  $r = 4''$  to the nucleus, corresponding to the inner  $\sim 1$  kpc of the galaxy. This value is also typical of  $Z$ -gradients mapped from the radial variations of the O abundances in HII regions in galactic disks (e.g., Vila-Costas & Edmunds 1992 and references therein). To convert this gradient to a  $W$ -gradient we used the results of Jablonka, Alloin & Bica (1992). We adopted their calibration for an old, globular cluster population, corresponding to the steepest  $W$ - $Z$  relation, thus resulting in the largest possible  $W$ -variations for a fixed  $Z$ -gradient.

This exercise resulted in the following variations of the  $W$ s due to a  $Z$ -gradient:  $\Delta W(\text{CaK}) = 1.2 \text{ \AA}$ ,  $\Delta W(\text{G-band}) = 0.8 \text{ \AA}$  and  $\Delta W(\text{Mg}) = 0.5 \text{ \AA}$ . Given that the assumptions above were all made in the sense of maximizing the effects of a  $Z$ -gradient, these variations should be regarded as upper limits. These are small variations, being of the same order of the errors in  $W$  (§3.1). The net variations with respect to the typical values of  $W$  found in our off-nuclear extractions ( $\sim 13 \text{ \AA}$  for Ca K and  $\sim 8 \text{ \AA}$  for both G-band and Mg) would correspond to changes of, at most, 10% in  $W(\text{Ca K})$ , 8% in  $W(\text{G-band})$  and 6% in  $W(\text{Mg})$ .

These results, while certainly not closing the question, seem to indicate that  $Z$ -gradients do not constitute a serious caveat to the interpretation of  $W$ -profiles in AGN. Only galaxies with a FC weaker than 6–10% could have a dilution

of the metal lines masked by the  $Z$ -gradient. Whilst we do not think that a compensation of the effects of a FC and a  $Z$ -gradient provides a viable interpretation for the ubiquitous absence of dilution in our sample galaxies, particularly in Seyferts 2, further investigations on the strength and detectability of  $Z$ -gradients in active galaxies would clearly be welcome, as this issue also bears on the question of whether an off-nuclear extraction provides a better starlight template for the nuclear stellar population than a normal galaxy (§5.1).

### 5.3 Color gradients

The continuum ratios in the sample galaxies exhibit an interesting radial behavior. As seen in Figs. 3–44, the  $F_{5870}/F_{4020}$  and  $F_{4630}/F_{3780}$  ratios very often peak in the nucleus, indicating a *redder* continuum. This seems to be an extremely ubiquitous behavior. The two kinds of objects which do not follow this rule are those containing nuclear starbursts, namely, NGC 1598, 6221, 5135, 7130, and broad-lined objects, the most extreme examples being MCG -02-33-034 and Pictor A. In particular, *all* Seyfert 2s, with the exception of NGC 5643 which shows a complex color profile, have nuclei redder than the extranuclear regions. This effect is not an artifact of our pseudo continuum determination, as we verified that the color-profiles are nearly identical if instead of the pseudo-continuum one defines line-free bands close to the pivot points to compute mean fluxes and flux ratios.

This is a somewhat surprising result, given that the

general prejudice is that AGN are bluer than normal galaxies, and as such they should also be bluer than their own bulges. On the other hand, if taken as evidence of reddening, the color profiles would fit in to the currently favored view that the nuclear regions of Seyfert 2s are rich in dust. Some support to this interpretation comes from the behavior of the Na line (partially produced in interstellar medium), whose W profiles in some galaxies, notably ESO 417-G6, NGC 1386, ESO 362-G8, NGC 6300 and NGC 7582, peaks in the nucleus, mimicking the color profiles. Examination of the radial behavior of the  $H\alpha/H\beta$  emission line ratio would provide a test of this interpretation.

Another intriguing result was found from the comparison of the stellar population templates inferred from the Ws with those inferred from the continuum ratios for the Seyfert 2s. With few exceptions, the off-nuclear colors indicate a spectral template *bluer* than that indicated by the absorption lines. At present we cannot give a clear explanation for this apparent contradiction, but we speculate on two possible interpretations. (1) The effect is due to a strong contribution from metal rich (thus strong lined) intermediate age (thus blue) stars, a population not well represented by any of templates S1–S7. This would be a genuine stellar population effect. (2) The blue continuum is due to a scattered AGN component while the absorption lines originate in a metal rich population. This would result in an *extended dilution* of the stellar features, whose Ws would therefore be underestimated, leading to the incorrect attribution of a spectral template less metallic than the actual population. Detailed modeling will be required to test these possibilities.

## 6 SUMMARY

We have reported the results of a high signal-to-noise ratio long slit spectroscopy study of 39 active galaxies and 3 normal galaxies. The run of stellar absorption lines and continuum colors with distance from the nucleus was investigated using a consistent methodology, aiming a global characterization of the stellar populations and the detection of a nuclear FC through the dilution of conspicuous absorption lines with respect to off-nuclear extractions. Our results can be summarized as follows.

(1) Radial variations of the stellar populations were detected in most cases. Star-forming rings, in particular, were found to leave clear imprints in the equivalent widths and color profiles.

(2) The stellar populations in the inner arcseconds of active galaxies are varied, as inferred from the wide spread of equivalent widths and colors measured in this work. This fact alone raises serious doubts as to whether it is appropriate to use a single starlight template to evaluate and remove the stellar component from AGN spectra.

(3) The equivalent width profiles were used to measure the dilution of the absorption lines in the nucleus with respect to off-nuclear spectra. Dilution by a nuclear FC was detected in most broad lined objects in the sample.

(4) Galaxies undergoing star-formation in their nuclei, including composite starburst + Seyfert 2 objects, also show dilution of the nuclear absorption lines. The dilution in these cases is due to young stars, not to a FC. These galaxies also

show a clear color gradient, their nuclei being bluer than off-nuclear regions.

(5) About 50% of the Seyfert 2s in the sample show no signs of dilution of their absorption lines in the nucleus, indicating that a FC, if present, contributes less than 10% of the total flux in the optical range. Possible consequences to the (controversial) nature of the FC in Seyfert 2s were discussed.

(6) All but one of the Seyfert 2s present a color gradient in the sense that the spectrum gets *redder* as we approach the nucleus, indicative of the presence of dust.

(7) There is an apparent discrepancy between the spectral templates assigned from the equivalent widths of the absorption lines and from the continuum colors, an effect observed in the off-nuclear spectra of most Seyfert 2s in the present sample. Tentative interpretations involving either a stellar population effect or an extended blue continuum were briefly outlined.

**Acknowledgments:** We thank Dr. E. Bica for useful discussions and remarks on an early version of this manuscript. HRS acknowledges the hospitality of the Department of Physics at Florianópolis. Support from FAPEU-UFSC is also duly acknowledged. RCF work was partially supported by CNPq under grant 300867/95-6. This research has made use of the NASA/IPAC Extragalactic Database (NED) which is operated by the Jet Propulsion Laboratory, CALTECH, under contract with the National Aeronautics and Space Administration.

## REFERENCES

- Antonucci, R. R. J. 1984, ApJ, 278, 499
- Antonucci, R. R. J. 1993, ARA&A, 31, 473
- Aretxaga, I., Terlevich, R. 1994, MNRAS, 269, 462
- Baum, S. A., Heckman, T., Brindle, A., van Breugel, W. & Miley, G. 1988, ApJS, 68, 643
- Baum, S. A. & Heckman, T. 1989, ApJ, 336, 681
- Bica, E. 1988, A&A, 195, 76
- Bica, E. & Alloin, D. 1986, A&A, 166, 83
- Bica, E., Pastoriza, M. G., Maia, M., Da Silva, L. A. L. & Dottori, H. 1991, AJ, 102, 1702
- Binette, L., Wilson, A. S. & Storchi-Bergmann, T. 1996, A&A, 312, 365
- Bonatto, C. J., Bica, E. & Alloin 1989, A&A, 226, 23
- Buta, R. 1986, ApJS, 61, 631
- Buta, R. 1987, ApJS, 64, 383
- Buta, R., Crocker D. A. 1992 AJ, 103, 1804
- Christiansen, W. N., Frater, R. H., Watkinson, A., O’Sullivan, J. D. & Lockhart, I. A. 1977, MNRAS, 181, 183
- Cid Fernandes, R. 1996, Vistas in Astronomy, 40, 143
- Cid Fernandes, R. & Terlevich, R. 1992, in “Relationships between Starburst and Active galaxies”, Filippenko, A. (ed.), (ASP Conference Series), 241
- Cid Fernandes, R. & Terlevich, R. 1995, MNRAS, 272, 423
- Colbert, E. J. M., Baum, S. A., Gallimore, J. F., O’Dea, C. & Christensen, J. A. 1996, ApJ, 467, 551
- de Grijs, M. H. K., Keel, W. C., Miley, G. K., Goudfrooij, P. & Lub, J. 1992, A&AS, 96, 389
- Davies R. L., Sadler E. M., Peletier R. F. 1993, MNRAS, 262, 650
- De Robertis, M. M. & Osterbrock, D. E. 1986a, ApJ, 301, 98
- De Robertis, M. M. & Osterbrock, D. E. 1986b, ApJ, 301, 727
- Díaz, A. I. 1985, Ph.D. thesis, University of Sussex

- Díaz, A. I. 1992, in “Relationships between Starburst and Active galaxies”, Filippenko, A. (ed.), (ASP Conference Series), 181
- Fairall, A. P. 1988, MNRAS, 233, 691
- Fairall, A. P. 1981, MNRAS, 196, 417
- Ferland, G. J. & Osterbrock, D. E. 1986, ApJ, 300, 658
- Filippenko, A. V. & Halpern, J. P. 1984, ApJ, 285, 458
- Filippenko, A. V. & Sargent, W. L. W. 1985, ApJS, 57, 503
- Filippenko, A. V. & Sargent, W. L. W. 1988, ApJ, 324, 134
- Garcia-Vargas, M. L., Díaz, A. I., Terlevich, R. & Terlevich, E. 1990, Ap&SS, 171, 65
- Goodrich, R. W. & Veilleux, S. & Hill, G. J. 1994, ApJ, 422, 521
- Halpern, J. P. & Eracleous, M. 1994, ApJ, 433, L17
- Halpern, J. P. & Filippenko, A. V. 1984, ApJ, 285, 475
- Haniff, C. A., Wilson, A. S. & Ward, M. J. 1988, ApJ, 334, 104
- Harnett, J. I. 1987, MNRAS, 227, 887
- Heckman, T., Krolík, J., Meurer, G., Calzetti, D., Kinney, A., Koratkar, A., Leitherer, C., Robert, C. & Wilson, A. S. 1995, ApJ, 452, 549
- Ho, L. C., Filippenko, A. V. & Sargent, W. L. W. 1993, ApJ, 417, 63
- Huchra, J. P., Wyatt, W. F. & Davis, M. 1982, AJ, 87, 1628
- Jablonka P., Alloin D., Bica E. 1990, A&A, 235, 22
- Kay, L. E. 1994, ApJ, 430, 196
- Keel, W. C. 1983, ApJ, 269, 466
- Kinney, A. L., Bohlin, R. C., Calzetti, D., Panagia, N. & Wyse, R. F. G. 1993, ApJS, 86, 5
- Kinney, A. L., Antonucci, R. R. J., Ward, M. J., Whittle, M. & Wilson, A. S. 1991, ApJ, 377, 100
- Koski, A. T. 1978, ApJ, 223, 56
- Kruper, J. S., Urry, C. M., Canizares, C. R. 1990, ApJS, 74, 347
- Kukula, M. J., Pedlar, A., Baum, S. A. & O’Dea, C. 1995, MNRAS, 26, 1262
- Lípari, S., Tsvetanov, Z. & Macchetto, F. 1993, ApJ, 405, 186
- Malkan, M. A. & Filippenko, A. V. 1983, ApJ, 275, 477
- Marshall, F. E., Boldt, C. A., Holt, S. S., Mushotzky, R. F., Pravdo, S. H., Rotschild, R. E., Serlemitsos, P. J. 1979, ApJS, 40, 657
- Martin, P. G., Thompson, I. B., Maza, J. & Angel, J. R. P. 1983, ApJ, 266, 470
- Miller, J. S. & Goodrich, R. W. 1990, ApJ, 355, 456
- Morris, S., Ward, M., Whittle, M., Wilson, A. S. & Taylor, K. 1985, MNRAS, 216, 193
- Mouri, H., Taniguchi, Y., Kawara, K. & Nishida, M. 1989, ApJ, 346, L73
- Mulchaey, J. S., Wilson, A. S. & Tsvetanov, Z. 1996, ApJS, 102, 309
- Osterbrock, D. E. & De Robertis, M. M. 1985, PASP, 97, 1129
- Pence, W. D. & Blackman, C. P. 1984, MNRAS, 207, 9
- Phillips, M. M. 1979, ApJ, 227, L121
- Phillips, M. M., Charles, P. A. & Baldwin, J. A. 1983, ApJ, 266, 485
- Phillips, M. M., Jenkins, C. R., Dopita, M. A., Sadler, E. M. & Binette, L. 1986, AJ, 91, 1062
- Phillips, M. M., Pagel, B. E. J., Edmunds, M. G. & Díaz, A. I. 1984, MNRAS, 210, 701
- Pogge, R. W. 1989a, ApJ, 345, 730
- Pogge, R. W. 1989b, ApJS, 71, 433
- Pogge, R. W. & De Robertis, M. M. 1993, ApJ, 404, 563
- Ruiz, M., Rieke, G. H. & Schmitt, G. D. 1994, ApJ, 423, 608
- Saikia, D. J., Pedlar, A., Unger, S. W. & Axon, D. J. 1994, MNRAS, 270, 46
- Schmidt, A. A., Bica, E. & Alloin, D. 1990, MNRAS, 243, 620
- Schmitt, H. R. 1994, Msc. Thesis, Universidade Federal do Rio Grande do Sul, Brazil
- Schmitt, H. R., Bica, E. & Pastoriza, M. G. 1996, MNRAS, 278, 965
- Schmitt, H. R. & Kinney, A. L. 1996, ApJ, 463, 497
- Schmitt, H. R. & Storchi-Bergmann, T. 1995, MNRAS, 276, 592
- Schmitt, H. R., Storchi-Bergmann, T. & Baldwin, J. A. 1994, ApJ, 423, 237
- Sekiguchi, K. & Menzies, J. W. 1990, MNRAS, 245, 66
- Sérsic, J. L. & Pastoriza, M. 1965, PASP, 77, 287 (SP65)
- Sérsic, J. L. & Pastoriza, M. 1967, PASP, 79, 152 (SP67)
- Shields, J. C. & Filippenko, A. V. 1990, AJ, 100, 1034
- Stauffer J. R., ApJ, 262, 66
- Simpson, C., Ward, M. J. & Wilson, A. S. 1995, ApJ, 454, 683
- Storchi-Bergmann, T., Baldwin, J. A. & Wilson, A. S. 1993, ApJ, 410, L11
- Storchi-Bergmann, T., Bica, E. & Pastoriza, M. G. 1990, MNRAS, 245, 749
- Storchi-Bergmann, T. & Bonatto, C. J. 1991, MNRAS, 250, 138
- Storchi-Bergmann, T., Eracleous M., Halpern J., Wilson A., Filippenko A. 1995a, ApJ, 443, 617
- Storchi-Bergmann, T., Kinney, A. L. & Challis, P. 1995b, ApJS, 98, 103
- Storchi-Bergmann, T. & Pastoriza, M. G. 1989, ApJ, 347, 195
- Storchi-Bergmann, T., Rodriguez-Ardila, A., Schmitt, H. R., Wilson, A. S. & Baldwin, J. A. 1996a, ApJ, 472, 83
- Storchi-Bergmann, T., Wilson, A. S. & Baldwin, J. A., 1996b, ApJ, 460, 252
- Storchi-Bergmann, T., Wilson, A. S., Mulchaey, J. S. & Binette, L. 1996, A&A, 312, 357
- Storchi-Bergmann T., Bica E., Kinney A., Bonatto C. 1997, MNRAS, submitted
- Tadhunter, C. N., Fosbury, R. A. E. & Quinn, P. J. 1989, MNRAS, 240, 225
- Terlevich, R., Melnick, J., Mesagosa, J., Moles, M. & Copetti, M. V. F. 1991, A&AS, 91, 285
- Thuan, T. X. 1984, ApJ, 281, 126
- Tran, H. D. 1995a, ApJ, 440, 565
- Tran, H. D. 1995b, ApJ, 440, 578
- Tran, H. D. 1995c, ApJ, 440, 597
- Tran, H. D., Miller, J. S. & Kay, L. E. 1992, ApJ, 397, 452
- Ulvestad, J. S. & Wilson, A. S. 1984a, ApJ, 278, 544
- Ulvestad, J. S. & Wilson, A. S. 1984b, ApJ, 285, 439
- Ulvestad, J. S. & Wilson, A. S. 1989, ApJ, 343, 659
- Unger, S. W., Pedlar, A., Neff, S. G. & de Bruyn, A. G. 1984, MNRAS, 209, 15p
- Véron-Cetty, M.-P., Véron, P. 1986, A&AS, 66, 335
- Véron, M. P., Véron, P. & Zuiderwijk, E. J. 1981, A&A, 98, 34
- Weaver, K. A., Wilson, A. S. & Baldwin, J. A. 1991, ApJ, 366, 50
- Winge C., Peterson B. M., Horne K., Pogge R. W., Pastoriza M., Storchi-Bergmann T. 1995, ApJ, 445, 680
- Winkler, H. 1992, MNRAS, 257, 677
- Winkler, H., Glass, I. S., van Wyk, F., Marang, F., Spencer Jones, J. H., Buckley, D. A. H. & Sekiguchi, K. 1992, MNRAS, 257, 659
- Wood, K. S., Meekins, J. F., Yentis, D. J., Smathers, H. W., McNutt, D. P., Bleach, R. D., Byran, E. T., Friedman, H., Meidav, M. 1984, ApJS, 56, 507
- Yee, H. K. C. 1980, ApJ, 241, 894

This figure "FIG1.jpg" is available in "jpg" format from:

<http://arxiv.org/ps/astro-ph/9801309v1>

This figure "FIG\_ZOOMab.jpg" is available in "jpg" format from:

<http://arxiv.org/ps/astro-ph/9801309v1>

This figure "FIG\_ZOOMcd.jpg" is available in "jpg" format from:

<http://arxiv.org/ps/astro-ph/9801309v1>